

Choosing Wavelet Methods, Filters, and Lengths for Functional Brain Network Construction

Zitong Zhang^{a,b}, Qawi K. Telesford^b, Chad Giusti^{b,c}, Kelvin O. Lim^d,
Danielle S. Bassett^{b,e}

^a*Department of Biomedical Engineering, Tsinghua University, Beijing 100084, China*

^b*Department of Bioengineering, University of Pennsylvania, Philadelphia, PA 19104, USA*

^c*Warren Center for Network and Data Sciences, University of Pennsylvania, PA 19104, USA*

^d*Department of Psychiatry, University of Minnesota, Minneapolis, MN 55455, USA*

^e*Department of Electrical and Systems Engineering, University of Pennsylvania, Philadelphia, PA 19104, USA*

Keywords: Wavelet Filters, Functional brain network, fMRI, Network diagnostics

Abstract Wavelet methods are widely used to decompose fMRI, EEG, or MEG signals into time series representing neurophysiological activity in fixed frequency bands. Using these time series, one can estimate frequency-band specific functional connectivity between sensors or regions of interest, and thereby construct functional brain networks that can be examined from a graph theoretic perspective. Despite their common use, however, practical guidelines for the choice of wavelet method, filter, and length have remained largely undelineated. Here, we explicitly explore the effects of wavelet method (MODWT vs. DWT), wavelet filter (Daubechies Extremal Phase, Daubechies Least Asymmetric, and Coiflet families), and wavelet length (2 to 24) – each essential parameters in wavelet-based methods – on the estimated values of network diagnostics and in their sensitivity to alterations in psychiatric disease. We observe that the MODWT method produces less variable estimates than the DWT method. We also observe that the length of the wavelet filter chosen has a greater impact on the estimated values of network diagnostics than the type of wavelet chosen. Furthermore, wavelet length impacts the sensitivity of the method to detect differences between health and disease and tunes classification accuracy. Collectively, our results suggest that the choice of wavelet method and length significantly alters the reliability and sensitivity of these methods in estimating values of network diagnostics drawn from graph theory. They furthermore demonstrate the importance of reporting the choices utilized in neuroimaging studies and support the utility of exploring wavelet parameters to maximize classification accuracy in the development of biomarkers of psychiatric disease and neurological disorders.

1. Introduction

The use of functional neuroimaging has gained considerable popularity over the last two decades as it provides a noninvasive approach for studying the brain (Biswal et al., 1995). Although a relatively recent addition to the methods available for analyzing neuroimaging data, network science has enhanced our understanding of the brain as a complex system. Rooted in techniques derived from graph theory, brain network analysis has been used to study neural diseases (Boersma et al., 2013), aging (Geerligs et al., 2014), and cognitive function (Mantzaris et al., 2013). The graph theory formalism defines a network by nodes (brain regions) and edges (connections between brain regions). In neuroimaging studies, nodes can describe atlas-based regions (Tzourio-Mazoyer et al., 2002b) or voxels (Eguiluz et al., 2005; van den Heuvel et al., 2008), and edges can define physical connections, in the case of anatomical networks (Sporns et al., 2002, 2007; Hagmann et al., 2008), or functional connections, which describe a statistical relationship between the activity time series of two nodes (Honey et al., 2007, 2009).

The goal of generating a brain network is straightforward: to use network science to understand the structure and function of the brain. Most studies report basic graph diagnostics, which include features of individual nodes (e.g., node centralities), features of groups of nodes (e.g., community structure or modularity), or features of the whole brain (e.g., global efficiency). Network analysis can also be used to explore fundamental principles of brain network organization, including small-world architecture (Humphries and Gurney, 2008), cost-efficiency (Bullmore and Sporns, 2012), and reconfiguration dynamics (Bassett et al., 2011; Hutchison et al., 2013). Across these studies, the main focus is to understand the organization of nodes and edges in the network. However, what has received less attention is the methodology used to define the functional relationships between nodes. In the context of functional brain networks, popular methods to define statistical relationships between regional activity time series include Pearson’s correlation coefficient (Zalesky et al., 2012), coherence (Peters et al., 2013), wavelet correlation (Achard et al., 2006a), and wavelet coherence (Bassett et al., 2011, 2013c,a; Mantzaris et al., 2013; Bassett et al., 2014, 2015); a less common method is the cross-sample entropy (Pritchard et al., 2014).

Wavelet-based methods have significant advantages in terms of denoising (Fadili and Bullmore, 2004), robustness to outliers (Achard et al., 2006a), and utility in null model construction (Breakspear et al., 2004). Moreover,

wavelet-based methods facilitate the examination of neurocognitive processes at different temporal scales without the edge effects in frequency space that accompany traditional band pass filters (Percival and Walden, 2000). But perhaps the most compelling argument in support of wavelets (Achard and Bullmore, 2007a) derives from the fact that cortical fMRI time series display slowly decaying positive autocorrelation functions (also known as long memory) (Maxim et al., 2005; Wink et al., 2006). This feature undermines the utility of measuring functional connectivity between a pair of regional time series using a correlation (time domain) or coherence (frequency domain), because both time- and frequency-domain measures of association are not properly estimable for long memory processes (Beran, 1994). In contrast, wavelet-based methods provide reliable estimates of correlation between long memory time series (Whitcher et al., 2000a; Gencay et al., 2001) derived from fMRI data (Achard and Bullmore, 2007a; Bullmore et al., 2004; Achard et al., 2008). Based on these advantages, wavelet-based estimates of functional connectivity have provided extensive insights into brain network organization in health (Achard et al., 2006b), aging (Achard and Bullmore, 2007b), neurological disorders (Supekar et al., 2008), sleep (Spoormaker et al., 2010), and cognitive performance (Gießing et al., 2013).

Despite the utility of wavelet-based approaches for estimating functional connectivity, fundamental principles to guide the performance of wavelet-based methods remain largely undefined. This lack of guidelines is apparent in the wide range of wavelet methods, filters, and lengths utilized in graph theoretical neuroimaging studies, which hampers comparability and reproducibility of subsequent findings. Here we explore the use of different wavelet methods (MODWT vs. DWT), filters (Daubechies Extremal Phase, Daubechies Least Asymmetric, and Coiflet families), and lengths (2–24) to determine their implications for the estimated values of network diagnostics. We quantify diagnostic variability, sensitivity, and utility in classifying resting state functional connectivity patterns extracted from people with schizophrenia and healthy controls using a previously-published fMRI data set (Bassett et al., 2012). Our results demonstrate that wavelet method and length impact subsequent network diagnostics, but wavelet type has little effect. Based on our findings, we suggest that researchers use MODWT methods with a wavelet length of 8 or greater, and carefully report their choices to enhance comparability of results across studies.

2. Materials and Methods

2.1. Ethics Statement

All human subjects provided informed consent according to a protocol approved by the Institutional Review Board at the University of Minnesota.

2.2. fMRI data acquisition and preprocessing

Resting-state fMRI data from 29 healthy controls (11 females; age 41.1 ± 10.6 (SD)) and 29 participants with chronic schizophrenia (11 females; age 41.3 ± 9.3 (SD)) were included in this analysis (See (Camchong et al., 2011) for detailed characteristics of participants and imaging data). A Siemens Trio 3T scanner was used to collect the imaging data, including a 6-min (TR=2 secs; 180 volumes) resting-state fMRI scan, in which participants were asked to remain awake with their eyes closed, a field map scan, and a T1 MPRAGE whole brain volumetric scan. The fMRI data were preprocessed using FEAT (FMRIB’s Software Library in FSL) with the following pipeline: deletion of the first 3 volumes to account for magnetization stabilization; motion correction using MCFLIRT; B0 fieldmap unwarping to correct for geometric distortion using acquired field map and PRELUDE+FUGUE52; slice-timing correction using Fourier-space time-series phase-shifting; non-brain removal using BET; regression against the 6 motion parameter time courses; registration of fMRI to standard space (Montreal Neurological Institute-152 brain); registration of fMRI to high resolution anatomical MRI; registration of high resolution anatomical MRI to standard space. Importantly, the two groups had similar mean RMS motion parameters: Two-sample t-tests of mean RMS translational and angular movement were both not significant ($p = 0.14$ and $p = 0.12$, respectively).

2.3. Statistical analysis

All calculations were done in MATLAB R2013b (The MathWorks Inc.). We used the WMTSA Wavelet Toolkit for MATLAB (<http://www.atmos.washington.edu/~wmtsa/>) to perform the wavelet decompositions, and we used the Brain Connectivity Toolbox (<https://sites.google.com/site/bctnet/>) to estimate values for network diagnostics.

2.4. Network construction

We extracted average time series for each participant from 90 of the 116 anatomical regions of interest (ROIs) defined by the AAL atlas (Tzourio-Mazoyer et al., 2002a) covering the whole brain and including cortical and subcortical regions but excluding the cerebellar regions and vermis. We performed a battery of wavelet decompositions on each regional mean time series by varying wavelet method (DWT vs. MODWT), wavelet filter (Daubechies Extremal Phase, Daubechies Least Asymmetric, and Coiflet families), and wavelet length (2–24). In prior literature, both the discrete wavelet transform (DWT) and the maximal overlap discrete wavelet transform (MODWT) methods have been used to create functional connectivity matrices (see (Deuker et al., 2009) and (Vertes et al., 2012) respectively for examples). DWT is an orthogonal transform, just as the discrete Fourier transform (DFT); MODWT adds redundancy to DWT, and can be thought as a non-downsampled version of it (Percival and Walden, 2000).

Wavelet filter and length alter the symmetry and shape of the wavelet (see Fig. 1). To examine the effect of wavelet filter, we apply Daubechies Extremal Phase, Daubechies Least Asymmetric, and Coiflet families (Percival and Walden, 2000), which together constitute the most widely used orthogonal and compactly supported types of wavelet filters. We abbreviate these three filters types as D (Daubechies Extremal Phase), LA (Daubechies Least Asymmetric), and C (Coiflet). To examine the effect of wavelet length, we vary the length of the filter from 2 to 24. We refer to each wavelet type and length together; for example, D_4 refers to the Daubechies Extremal Phase filter that has a length of 4.

Consistent with prior work (Achard et al., 2006a; Fornito et al., 2011), we apply this battery of wavelet decompositions to each regional mean time series and extract wavelet coefficients for the first four wavelet scales, which in this case correspond to the frequency ranges 0.125~0.25 Hz (Scale 1), 0.06~0.125 Hz (Scale 2), 0.03~0.06 Hz (Scale 3), and 0.015~0.03 Hz (Scale 4). For each subject, wavelet method (DWT vs. MODWT), wavelet filter (Daubechies Extremal Phase, Daubechies Least Asymmetric, and Coiflet families), and wavelet length (2–24), we constructed a correlation matrix whose ij^{th} elements were given by the estimated wavelet correlation between the wavelet coefficients of brain region i and the wavelet coefficients of brain region j .

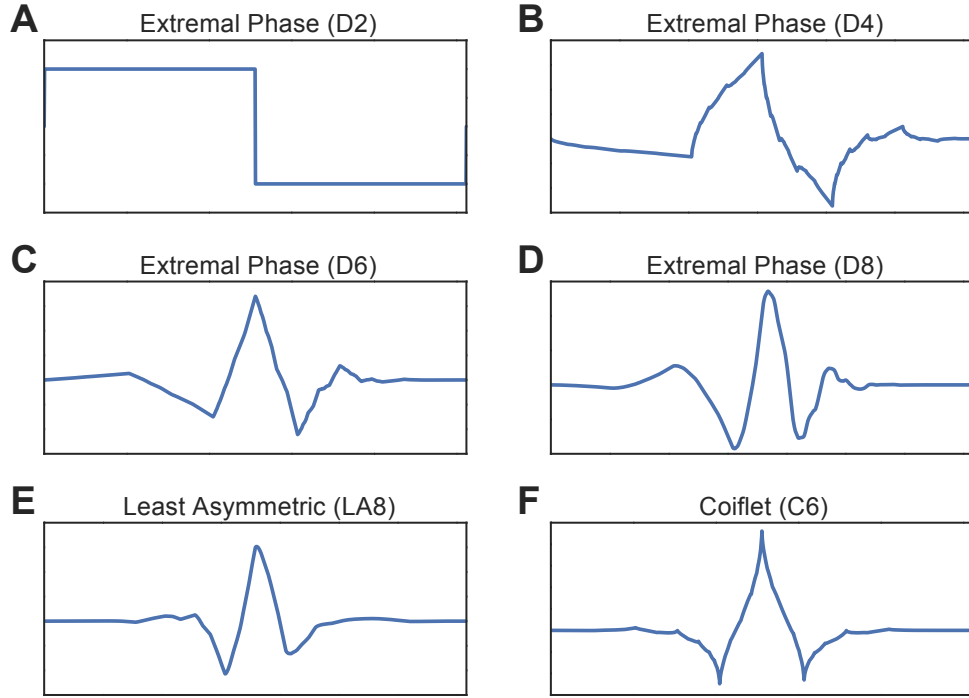


Figure 1: **Example Wavelet Functions of Filters From Each Filter Type.** (A–D) Daubechies Extremal Phase filter. (A) Filter with length 2. (B) Filter with length 4. (C) Filter with length 6. (D) Filter with length 8. (E) Daubechies Least Asymmetric filter with length 8. (F) Coiflet filter with length 6.

2.5. Network diagnostics

We characterized the organization of each functional connectivity matrix using both weighted and binary network diagnostics. To examine simple properties of the correlation matrix itself, we followed (Lynall et al., 2010a; Bassett et al., 2012) and calculated (i) the mean correlation coefficient of the matrix as the average of the upper triangular elements of the matrix, and (ii) the variance of the correlation coefficients of the matrix as the variance of the upper triangular elements of the matrix.

To examine the topological properties of each functional connectivity matrix, we performed a cumulative thresholding approach (Bassett et al., 2012) by which we thresholded each matrix to maintain the strongest edges, giving a binary undirected network that has a density of 30% (see the SI for examination of other thresholds). The choice of this threshold is based on a large and growing literature demonstrating small-world attributes of neuroimaging-based brain networks thresholded to retain this density (Achard and Bullmore, 2007a; Achard et al., 2006a; Deuker et al., 2009; Lynall et al., 2010a). On this thresholded binary matrix, we calculated several network diagnostics, including the clustering coefficient, characteristic path length, global efficiency, local efficiency, modularity, and number of communities. See the Appendix for mathematical definitions of these diagnostics.

The maximization of modularity requires the investigator to make several methodological choices (Bassett et al., 2013b). Due to the heuristic nature of the Louvain algorithm (Blondel et al., 2008) used in maximizing the modularity quality function (Newman, 2006b) and the degeneracy of the modularity landscape (Good et al., 2010), we performed 20 optimizations of Q for each functional connectivity matrix. The modularity values that we report are the mean values over these 20 optimizations. We also constructed a consensus partition (Lancichinetti and Fortunato, 2012) from these optimizations using a method that compares the consistency of community assignments to that expected in a null model (Bassett et al., 2013b).

2.6. Classification between healthy controls and schizophrenia patients

To inform the utility of various wavelet methods, filters, and lengths in neuroimaging studies of functional brain network architecture, we performed a classification analysis in which we sought to classify functional connectivity matrices extracted from 29 healthy subjects from those extracted from 29 people with schizophrenia (Bassett et al., 2012). This particular

data set is well-suited to this study because it has been difficult to classify these two groups of subjects using binary networks constructed from traditional methods; the data set therefore offers a reasonable testbed for optimization of classification accuracy as a function of methodological variation. To perform this classification, we gathered all network diagnostics obtained in scale 2 (corresponding to the most commonly utilized frequency band for resting state network analyses (Lynall et al., 2010a; Bassett et al., 2012)), and used a classification algorithm referred to as the C5.0 algorithm (<http://www.rulequest.com/see5-info.html>) to generate decision trees to classify data from healthy controls versus people with schizophrenia. The C5.0 algorithm supports boosting, and is faster and more memory efficient than the previous C4.5 algorithm (Quinlan, 1993), which in turn is an extension of the earlier ID3 algorithm (Quinlan, 1986). We generated decision trees with 10-trial boosting and 6-fold cross validation. The boosting method, AdaBoost, allows us to generate multiple decision trees for a given set of training data and combine them for better classification while avoiding overfitting (Freund et al., 1999). Utilizing the cross validation procedure, we randomly divided all of the subjects into 6 groups, and for each group, we trained a set of boosting decision trees on 5 groups and tested the decision trees on the remaining group. The results we report are the cumulative results across these 6 groups.

3. Results

In this section, we examine the effects of wavelet method (DWT vs. MODWT), wavelet filter (Daubechies Extremal Phase, Daubechies Least Asymmetric, and Coiflet families), and wavelet length (2–24) on (i) the estimated values of network diagnostics in healthy subjects, and (ii) the classification accuracy in distinguishing between functional connectivity matrices extracted from people with schizophrenia and healthy controls.

3.1. *The Effect of Wavelet Method: DWT vs. MODWT*

Both the DWT and the MODWT have previously been utilized to obtain wavelet coefficients for regional time series, prior to the construction of functional connectivity matrices representing graphs or networks (see (Deuker et al., 2009) and (Vertes et al., 2012) for recent examples). Here we performed a direct comparison between DWT and MODWT in terms of their effects on estimated network organization. In Fig. 2, we show the mean and

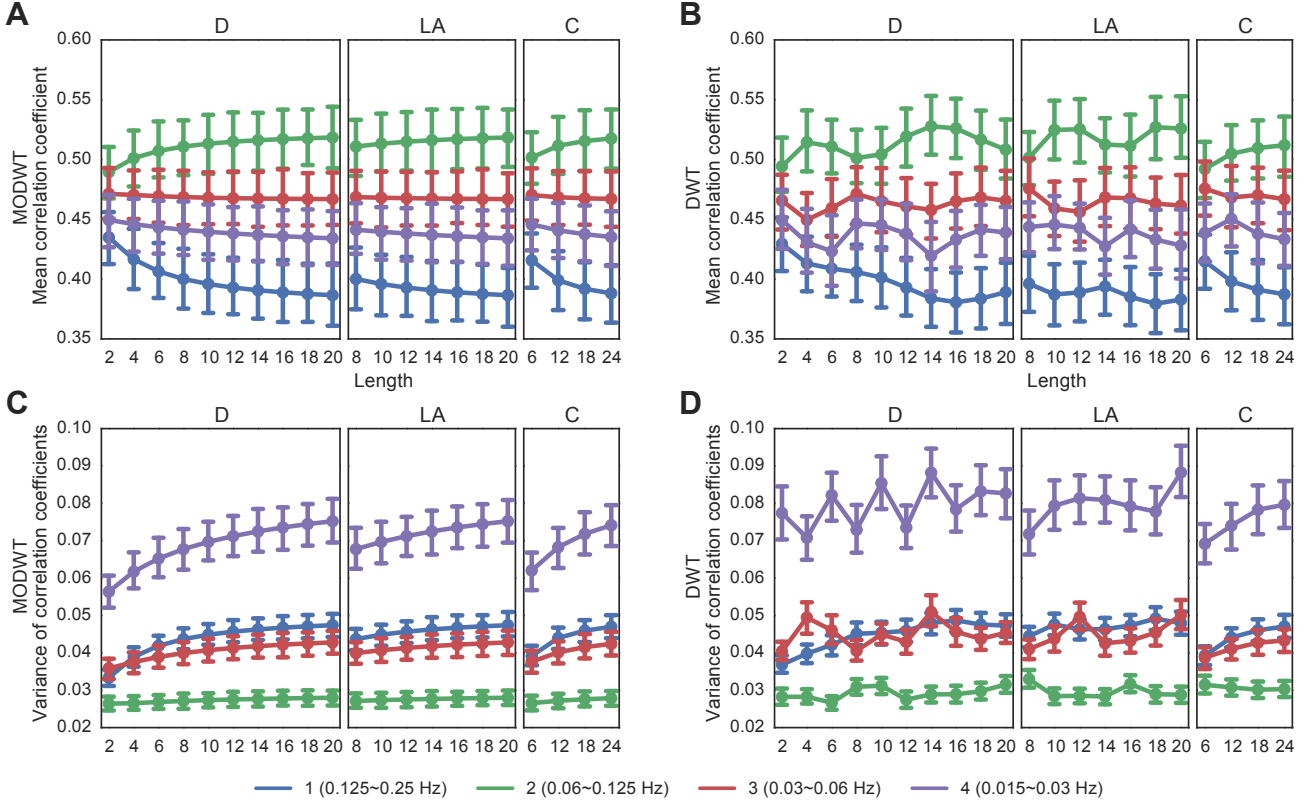


Figure 2: Effect of Wavelet Method on Mean and Variance of Correlation Coefficients (A, B) Mean correlation coefficients as a function of wavelet filter (Daubechies Extremal Phase, Daubechies Least Asymmetric, and Coiflet families) and wavelet length (2–24) observed when applying the (A) MODWT and (B) DWT. (C, D) Variance of correlation coefficients as a function of wavelet filter (Daubechies Extremal Phase, Daubechies Least Asymmetric, and Coiflet families) and wavelet length (2–24) observed when applying the (C) MODWT and (D) DWT. Wavelet scales are indicated by the color of the lines: scale 1 (approximately 0.125–0.25 Hz) is shown in blue, scale 2 (approximately 0.06–0.125 Hz) in green, scale 3 (approximately 0.03–0.06 Hz) in red, and scale 4 (approximately 0.015–0.03 Hz) in purple. Error bars indicate standard errors of the mean across 29 healthy subjects.

variance of the correlation coefficients of the functional connectivity matrices of healthy controls for all 3 wavelet filters, all 4 wavelet scales, and all wavelet lengths. In general, the shapes of the diagnostic versus wavelet length curves for both methods show qualitative similarities. We also observe that both DWT and MODWT give similar standard errors across subjects in the mean correlation coefficient and the variance of correlation coefficients.

Despite these gross qualitative similarities, we observe that the two methods differ in terms of (i) the variation of diagnostic values over wavelet lengths, and (ii) the magnitude of variance of correlation coefficients. Diagnostic values obtained using MODWT show a smooth change with increasing wavelet length, for all 3 wavelet filters and all 4 wavelet scales corresponding to different frequency bands (see Fig. 2 panels A and C). In contrast, diagnostic values obtained from DWT do not show smooth changes with increasing wavelet length (see Fig. 2 panels B and D). To quantify these observations, we calculated the sum of the absolute value of differences between diagnostics at consecutive lengths. For each scale and wavelet filter, we performed a paired t -test to test for differences in the mean. We found that – indeed – the variation of diagnostic values over wavelet lengths is significantly greater when using DWT than when using MODWT for all scales and all filters except scale 1 Coiflet; see Table 1.

Furthermore, the variance of correlation coefficients extracted using the MODWT method are smaller in magnitude than the variance of the correlation coefficients extracted using the DWT method (compare Fig. 2 panels C and D). To quantify this observation, we averaged the variance of the correlation coefficients over all wavelet lengths and filter types, separately for each scale. We performed a paired two-sided t -test to measure the difference between the average variance of correlation coefficients obtained using the DWT method versus those obtained using the MODWT method. We found that the average variance of the correlation coefficients was larger in the DWT case than in the MODWT case for all 4 wavelet scales: $t = 5.87$ and $p < 0.0001$ (Scale 1), $t = 8.89$ and $p < 0.0001$ (Scale 2), $t = 14.64$ and $p < 0.0001$ (Scale 3), and $t = 9.44$ and $p < 0.0001$ (Scale 4). Together these results are consistent with the theoretical notion that DWT provides more noisy estimates of structure than MODWT, and support the common preference in neuroimaging studies to use MODWT over DWT (Achard et al., 2006a).

Based on its reliable variation with wavelet length, we restrict ourselves to the study of network diagnostics extracted using the MODWT method

Scale	Filter type	Mean correlation coefficient		Variance of correlation coefficients	
		t	p	t	p
1	D	-6.00	0.0000	-3.93	0.0005
	LA	-5.38	0.0000	-5.97	0.0000
	C	0.94	0.3561	0.70	0.4920
2	D	-9.45	0.0000	-9.98	0.0000
	LA	-7.55	0.0000	-7.64	0.0000
	C	-3.32	0.0025	-2.47	0.0200
3	D	-6.98	0.0000	-7.36	0.0000
	LA	-10.01	0.0000	-8.52	0.0000
	C	-6.57	0.0000	-5.51	0.0000
4	D	-8.83	0.0000	-9.89	0.0000
	LA	-10.21	0.0000	-8.44	0.0000
	C	-9.99	0.0000	-5.32	0.0000

Table 1: **Variation of Diagnostic Values Over Wavelet Lengths** t -values and p -values for two-sample t -tests measuring the differences in the sum of the absolute value of differences between diagnostics at consecutive lengths obtained from the MODWT approach as opposed to the DWT approach ($df=28$ over the 29 healthy control subjects). Paired t -tests were performed separately for each filter type (“D” = Daubechies Extremal Phase, “LA” = Daubechies Least Asymmetric, and “C” = Coiflet) for each wavelet scale separately.

for the remainder of this paper.

3.2. The Effect of Wavelet Filter Type

In prior literature, many wavelet filters have been applied to the extraction of regional time series prior to functional brain network construction, including Daubechies (Deuker et al., 2009), and Least Asymmetric families (Jakab et al., 2013). Moreover, Coiflet wavelets have been shown to provide superior compression performance in magnetic resonance images (Abu-Rezq et al., 1999). Here we performed a direct comparison between Daubechies Extremal Phase, Daubechies Least Asymmetric, and Coiflet families in terms of their effects on estimated network organization. To isolate the effect of wavelet filter, we examine network diagnostics obtained using each filter family and a fixed wavelet length. In Fig. 3, we show representative results from a comparison of D6 and C6, and a comparison of D8 and LA8 in wavelet scale 2. Qualitatively, we observe no significant differences in network diagnostics estimated from different wavelet filters of the same wavelet length. To confirm this observation quantitatively, we use a sign test (due to the skewed distribution of the data) to test the hypothesis that the difference median is zero between the distributions of diagnostics for D6 and C6, and between the distributions of diagnostics for D8 and LA8. Consistent with our qualitative observations, we find no significant differences (as defined as $p < 0.05$ corrected for multiple comparisons using a conservative family-wise error correction). Note that we observe qualitatively similar results for other wavelet scales and other graph densities (see Supplemental Materials).

3.3. The Effect of Wavelet Filter Length

In prior literature, many wavelet lengths have been applied to the extraction of regional time series prior to functional brain network construction (for example see (Deuker et al., 2009) and (Jakab et al., 2013)). Here we performed a direct comparison between wavelet lengths 2 through 20 (Daubechies Extremal Phase), 8 to 20 (Daubechies Least Asymmetric), and 6 to 24 (Coiflet). Note these length choices were dictated by those available in the WMTSA toolbox (see Methods). Consistent with effects shown in Fig. 2, we observe that the length of the wavelet filter affects network diagnostics differently; some diagnostics are affected significantly (such as the modularity index), and other diagnostics are affected very little (such as the characteristic path length); see Fig. 4.

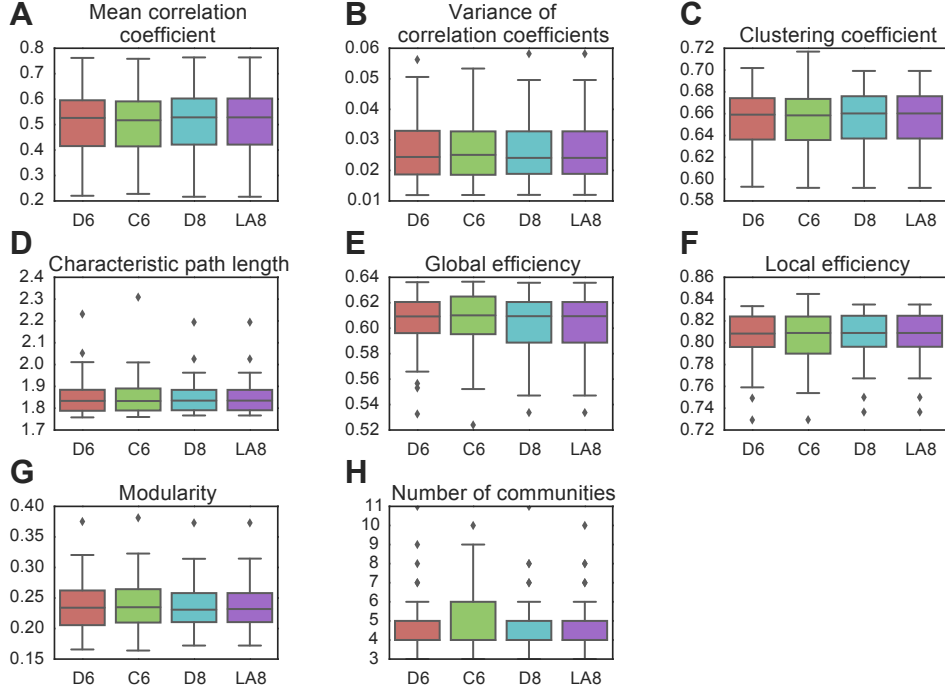


Figure 3: **Effect of Wavelet Filter on Network Diagnostics** in wavelet scale 2 between pairs of wavelet filters with the same length. (A, B) Weighted network diagnostics including (A) mean correlation coefficient and (B) variance of correlation coefficients. (C–F) Binary network diagnostics calculated at a graph density of 30% obtained through a cumulative thresholding procedure, including (C) the clustering coefficient, (D) characteristic path length, (E) global efficiency, (F) local efficiency, (G) modularity index Q , and (H) the number of communities. Boxplots indicate the median and quartiles of the data acquired from 29 health subjects. See Supplemental Materials for qualitatively similar results obtained at different scales and graph densities.

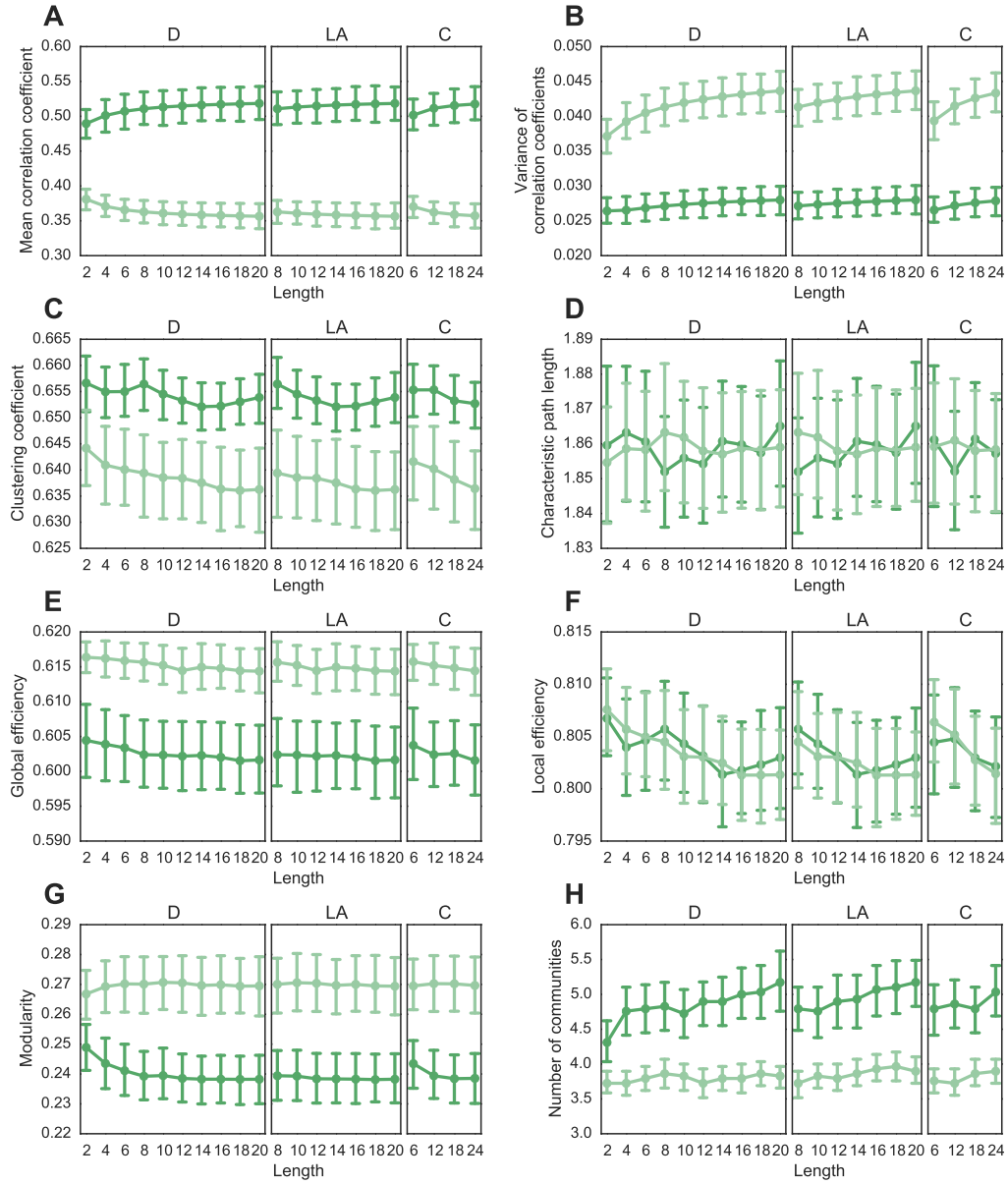


Figure 4: **Effect of Wavelet Length on Network Diagnostics** in wavelet scale 2 for all wavelet filters. (A, B) Weighted network diagnostics including (A) mean correlation coefficient and (B) variance of correlation coefficients. (C-F) Binary network diagnostics calculated at a graph density of 30% obtained through a cumulative thresholding procedure, including (C) the clustering coefficient, (D) characteristic path length, (E) global efficiency, (F) local efficiency, (G) modularity index Q , and (H) the number of communities. The more saturated curves represent data from the 29 healthy controls, while the less saturated curves represent data from 29 people with schizophrenia. Error bars depict standard errors of the mean across subjects. See Supplemental Materials for qualitatively similar results obtained at different wavelet scales.

To quantify the differential sensitivity of network diagnostics to wavelet length, we performed a set of repeated measures ANOVA, for each diagnostic and each type of wavelet filter. Here, wavelet filter length was treated as a categorical factor, and diagnostic type was treated as a repeated measure. For complete results for each of these ANOVAs, see Table 2. We observe that the mean and variance of correlation coefficients are significantly affected by wavelet length in all 3 wavelet filters. The characteristic path length and global efficiency are not significantly affected by wavelet length in any of the 3 wavelet filters. The clustering coefficient, local efficiency, modularity, and number of communities are affected by wavelet length in some but not all of the wavelet filters. These results demonstrate that network diagnostics are differentially sensitive to wavelet length, challenging the potential performance of meta-analyses that incorporate results obtained using different wavelet length and filters.

Note that we observe qualitatively similar results for other wavelet scales (see Supplemental Materials).

3.4. Classification in Psychiatric Disease

Finally, we asked whether different wavelet filters provide different degrees of statistical sensitivity or classification accuracy when seeking to distinguish between functional connectivity matrices extracted from healthy controls versus those extracted from people with schizophrenia.

To determine whether different wavelet filters provide different degrees of statistical sensitivity for group comparisons, we first visually inspect diagnostic values in wavelet scale 2 as a function of filter type and length (compare dark and light lines in Fig. 4). We observe that group differences in mean correlation coefficient, variance of correlation coefficients, clustering coefficient, modularity, and number of communities appear to be larger for longer wavelet lengths, across all three filter types. To quantify these observations, we performed a two-sample t -test between diagnostic values extracted from the two groups (patients vs. controls) for each filter type and length (see Fig. 5). In general, we observe that the p -values decreased with increasing wavelet length (as demonstrated by the increase in the minus log p -values in Fig. 5), suggesting that longer wavelets display greater statistical sensitivity to group differences in these data. This finding was particularly salient for the mean correlation coefficient, variance of the correlation coefficients, clustering coefficient, modularity and number of communities, consistent with our visual inspection of Fig. 4.

	Daubechies Extremal Phase (dF=9,252)		Daubechies Least Asymmetric (dF=6,168)		Coiflet (dF=3,84)	
	<i>F</i>	<i>p</i>	<i>F</i>	<i>p</i>	<i>F</i>	<i>p</i>
Mean	14.63	0.0000	16.12	0.0000	16.29	0.0000
correlation coefficient						
Variance of	4.57	0.0000	13.28	0.0000	8.62	0.0000
correlation coefficients						
Clustering coefficient	1.54	0.1333	4.47	0.0003	1.61	0.1937
Characteristic path length	0.37	0.9506	0.70	0.6503	0.53	0.6599
Global efficiency	0.95	0.4837	0.39	0.8852	1.18	0.3224
Local efficiency	1.60	0.1168	4.46	0.0003	1.32	0.2747
Modularity	6.88	0.0000	1.20	0.3089	5.07	0.0028
Number of communities	3.98	0.0001	3.41	0.0033	1.02	0.3898

Table 2: **Effect of Wavelet Length.** Results of Repeated Measures ANOVAs for network diagnostics extracted from 29 healthy controls at scale 2 and a graph density of 30%; wavelet length is treated as a factor and network diagnostic is treated as a repeated measure, separately for each wavelet filter type. Effects that are significant at $p < 0.05$, uncorrected, are shown in red.

In the SI, we explore the dependence of these results on methodological choices in network construction including the measure of functional connectivity (partial correlation, wavelet coherence, and the wavelet correlation used in the main manuscript), strength of edges (strongest versus weakest (Bassett et al., 2012; Schwarz and McGonigle, 2011)), and time series (wavelet details vs. wavelet coefficients). We observe that the effect of wavelet length is more salient (i) when using wavelet correlation than when using wavelet coherence or partial correlation, and (ii) when using the strongest 30% connections or 10% weakest connections than when using the 30% or 1% weakest connections. Results are consistent across the use of both wavelet details and wavelet coefficients. Based on prior work (Bassett et al., 2012), we speculate that the networks constructed from the 1% weakest connections display significant spatial localization and the networks that constructed from the 30% weakest connections display significant random structure, together overshadowing the potential effects of wavelet length on group differences.

We build on the above results drawn from parametric t -tests by applying non-parametric machine learning techniques to determine whether different wavelet filters provide different degrees of classification accuracy. Specifically, we generated decision trees (see Methods) to classify healthy controls and people with schizophrenia based on network diagnostics extracted from functional brain networks constructed from correlations in scale 2 wavelet coefficients. We observe that the classification accuracy ranged from approximately 63.8% to approximately 82.8%, the classification sensitivity ranged from approximately 65.5% to approximately 96.6%, and the classification specificity ranged from approximately 51.7% to 79.3% (see Fig. 6). The poorest classification accuracy and specificity occurred in *short* wavelets using the Daubechies Extremal Phase filter, and the best classification results occurred for relatively *long* wavelets using the Daubechies Least Asymmetric filter (LA14), which gave 82.8% accuracy and 96.6% sensitivity. These results support those obtained from the parametric t -test analysis, that larger wavelet lengths display greater statistical sensitivity to group differences in these data.

4. Discussion

Wavelet-based methods offer extensive benefits in time series analysis and functional brain network construction. These include denoising capabilities (Fadili and Bullmore, 2004), robustness to outliers (Achard et al., 2006a),

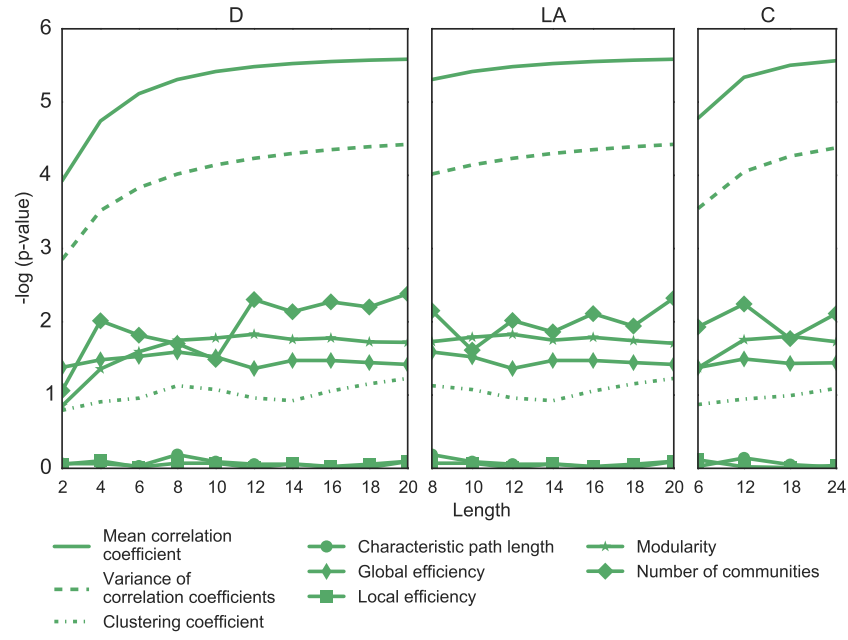


Figure 5: **Effect of Wavelet Filter Type and Length on Statistical Sensitivity in Group Comparisons.** Negative common logarithm of the p -values obtained from two-sample t -tests between diagnostic values extracted from healthy control networks versus those extracted from schizophrenia patient networks. Higher values indicate greater group differences and lower values indicate weaker group differences. Network diagnostics are calculated for wavelet scale 2; for results in wavelet scale 1, see the SI.

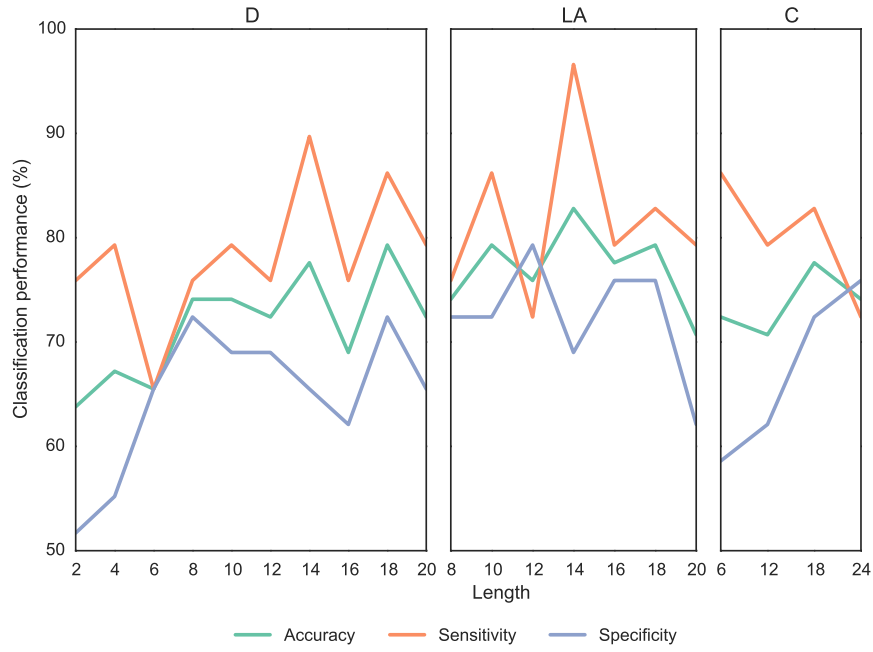


Figure 6: **Effect of Wavelet Filter Type and Length on Classification.** Classification accuracy, sensitivity, and specificity as a function of wavelet filter type and length. Results are based on decision trees (see Methods) and distinguish between healthy controls and people with schizophrenia based on network diagnostics computed in wavelet scale 2. Note that we have regarded schizophrenia as positive, which clarifies the direction of the sensitivity and specificity estimates.

utility in null model construction (Breakspear et al., 2004), frequency-specificity without edge effects (Percival and Walden, 2000), and accurate estimates of functional connectivity in long memory processes (Whitcher et al., 2000a; Gencay et al., 2001), such as those observed in fMRI time series (Maxim et al., 2005; Wink et al., 2006; Achard and Bullmore, 2007a; Bullmore et al., 2004; Achard et al., 2008). Yet despite their utility, fundamental principles to guide the performance of wavelet-based methods remain largely undefined, hampering comparability and reproducibility of wavelet-based functional connectivity studies. Here we explicitly fill this gap by exploring the use of different wavelet methods (MODWT vs. DWT), filters (Daubechies Extremal Phase, Daubechies Least Asymmetric, and Coiflet families), and lengths (2–24) and by determining their implications for the estimated values of functional network diagnostics and the sensitivity to group differences. We found that the MODWT produces less variable estimates than the DWT method, and that wavelet length significantly impacts network diagnostic values and sensitivity to group differences. Collectively, our results underscore the importance of reporting the choices utilized in neuroimaging studies and provide concrete recommendations for these choices in wavelet-based analyses.

In the remainder of this section, we translate our results into concrete recommendations for the field, and we close with a brief discussion of important future directions.

The Choice of Wavelet Method. The superior performance of MODWT in the context of the numerical experiments performed here is consistent with features of its theoretical construction (Whitcher et al., 2000b). First, and perhaps most importantly, MODWT is well defined for any signal length, making it statistically appropriate for the processing of arbitrary signals. In contrast, strictly speaking a DWT of level J_0 can be applied only to signals whose length is a multiple of 2^{J_0} , significantly limiting its application to signals of arbitrary lengths.¹ Second, while DWT is an orthogonal transform, MODWT is not. In fact, MODWT is highly redundant and invariant under ‘circular shift’ (Whitcher et al., 2000b; Percival and Walden, 2000). This feature of MODWT preserves the smooth time-varying structure in regional time series that is otherwise lost during the application of DWT. In the

¹In practice when applying the DWT to signals of arbitrary lengths, one can choose to avoid this issue – as we did in this study – by preserving at most one extra scaling coefficient at each level of wavelet decomposition.

context of human neuroimaging, analyses based on MODWT therefore more accurately reflect the dynamics of brain activity.

The Choice of Wavelet Filter Type and Length. Wavelet filter types offer differently shaped wavelets that can be applied to empirical time series in a wavelet decomposition. While there is a generally well-accepted notion that one should choose a wavelet that displays similar time-varying features to the time series at hand, we observed that wavelet filter type had very little influence on network diagnostics extracted from resting state fMRI signals. The much larger factor impacting network diagnostics was the wavelet length, which tunes the fine-scale detail of the wavelet shape: larger wavelet length provides smoother wavelets. In general, network diagnostics obtained using the Daubechies Extremal Phase wavelets changed more from wavelet lengths 2 to 6 than from lengths 6 to 20. These results are intuitive: the changes in wavelet smoothness are more apparent at shorter wavelet lengths than at larger wavelet lengths, and their impact on estimated wavelet coefficients should follow. From a reliability perspective, we would argue that one would wish to choose a wavelet of a relatively larger length, to ensure that one's results are (i) not sensitive to artifacts of jagged edges in the wavelet and (ii) are relatively robust to small perturbations in wavelet length. Yet, it is important to keep in mind that very large wavelet lengths may suffer from the following limitations: (i) more coefficients may be influenced by boundary conditions, (ii) a decrease in the degree of localization of the wavelet coefficients, (iii) an increase in computational burden (Percival and Walden, 2000). The ideal choice may therefore be a moderate length that retains the advantages of long wavelets without gaining any associated disadvantages.

Wavelets for Classification. In our methodological recommendations thus far, we have called on arguments of reliability, insensitivity to artifact, and decreased variability to support specific choices in wavelet-based functional network analysis. In a final analysis we further asked whether one can support these choices based on differential sensitivity to group differences in functional network architecture. In analyses based on scale 2 wavelet coefficients (corresponding to 0.06–0.125 Hz), the answer is clear: longer wavelet lengths provide increased sensitivity to group differences as measured both by parametric t -tests and non-parametric machine learning algorithms based on decision trees. Using these longer wavelets, we observe significantly greater classification accuracy, sensitivity, and specificity values than those previously observed in this same data set (Bassett et al., 2012), complementing

prior work demonstrating differences in spontaneous low-frequency (<0.1 Hz) fluctuations in BOLD signal (Bluhm et al., 2007; Fornito and Bullmore, 2010) and functional or structural network architecture (Lynall et al., 2010b; Liu et al., 2008; Liang et al., 2006; Skudlarski et al., 2010) between schizophrenia patients and healthy controls. Thus, in addition to their benefits in terms of sensitivity and robustness, longer wavelets offer greater sensitivity to group differences in this data set, supporting their choice in the performance of wavelet-based analyses of resting state fMRI data more broadly. We speculate that there might be some underlying structural difference between the two groups of subjects that is consistent among individuals, and that the longer wavelet lengths smooth small differences between individuals so that large-scale differences are clearer. More generally, we speculate that larger wavelet lengths are better able to distinguish group-level features, while shorter wavelets may better distinguish individual-level features.

Methodological Considerations. In general, our results point to the optimality of longer wavelets for functional network construction from low-frequency spontaneous fluctuations of the BOLD signal. However, it is interesting to note that for higher frequencies such as those probed by scale 1 coefficients (corresponding to 0.125–0.25 Hz), shorter wavelet lengths appear to provide better sensitivity to group differences; see the SI. The assessment of these higher frequencies is uncommon in functional network construction, due to their decreased power and relative lack of structured topological architecture (Achard et al., 2006b). Nevertheless, these results suggest that the optimal methodological choice for wavelet length might depend on the frequency band of interest, and therefore the properties of the signal being studied, an observation that might be particularly relevant in the assessment of functional networks in EEG and MEG data. Such a conclusion is supported by work identifying a variety of wavelet lengths and types as optimal for classification schemes in EEG signals (Subasi, 2007) and other complex systems (Palit et al., 2010; Semler et al., 2005). More work is therefore necessary to determine rules of thumb for wavelet analysis that are generalizable across frequency bands and imaging modalities.

We have exercised these methods on functional networks constructed using the AAL atlas applied to resting state fMRI data, which represent common choices in functional network analysis in both health and disease. It will be interesting in future to assess the utility of these methods in other parcellation schemes and in task-based data.

Future Directions. As a final note, it is worth pointing out that the wavelet decompositions utilized here build on procedures currently employed in the literature on functional brain network construction in an effort to provide the field with a few useful rules of thumb. However, other wavelet-based analysis techniques do exist – including wavelet packets, dual-tree complex wavelet transforms, and double-density DWT – that have not yet been applied to this problem, and it is not yet known whether these alternative techniques might provide complementary insights into whole-brain patterns of functional connectivity. It will be interesting in future to assess the utility of these alternative methods in reliably quantifying brain network organization and its alteration in disease states.

Appendix A. Relationship Between Sampling Frequency and Wavelet Scales

The frequency ranges extracted by a wavelet decomposition directly depend on the sampling frequency of the data. It is therefore important to delineate which features of our results are generalizable across data sets acquired with different sampling frequencies. The data used here was acquired with a TR of 2 s (a common choice), and therefore contains information up through the frequency 0.25 Hz. A wavelet decomposition of this signal affects consecutive scales in which the observed signal is repeatedly convolved with a wavelet filter (which behaves as a high-pass filter) and a related scaling filter (which behaves as a low-pass filter). The first four scales therefore correspond to the frequency ranges of approximately 0.125 – 0.25 Hz, 0.06 – 0.125 Hz, 0.03 – 0.06 Hz, and 0.015 – 0.03 Hz, respectively. We note that different sampling frequencies may be used in other experiments, and the applicability of our specific results will depend on the degree of overlap in the frequency ranges of wavelet scales. However, our approach and conclusions regarding (i) the benefits of MODWT, (ii) the utility of moderate wavelet lengths, and (iii) the relatively small effect of wavelet filter are expected to be more generally applicable.

Appendix B. Definitions of Network Diagnostics

1. Clustering coefficient C : The clustering coefficient is used to quantify the local clustering properties of the network. First, the local clustering

coefficient C_i of a node i can be defined as the fraction of actual edges between its neighbors (Watts and Strogatz, 1998):

$$C_i = \frac{\sum_{j \neq h} A_{ij} A_{ih} A_{jh}}{k_i(k_i - 1)},$$

where \mathbf{A} refers to the adjacency matrix, and k_i refers to the degree of node i . Then, the clustering coefficient of the network is defined as the mean of C_i over all nodes.

2. Characteristic path length L : The characteristic path length is defined as the length of the geodesic path between two vertices, averaged over all pairs of connected vertices:

$$L = \frac{\sum_m \sum_{ij \in \mathcal{V}_m} d_{ij}}{\sum_m n_m^2},$$

where \mathcal{V}_m refers to the set of vertices in connected component m , d_{ij} refers to the geodesic distance between node i and j , and n_m refers to the number of nodes in connected component m .

3. Global efficiency E_{glob} (Latora and Marchiori, 2001): The global efficiency has been interpreted as a measure of how effectively information can be exchanged through the network. It is defined as follows:

$$E_{\text{glob}} = \frac{1}{n(n-1)} \sum_{i \neq j} d_{ij}^{-1},$$

where n is the number of nodes in the network.

4. Local efficiency E_{loc} (Latora and Marchiori, 2001): The local efficiency of node i assesses the efficiency of the subgraph formed by the neighbors of i :

$$E_{\text{loc},i} = \frac{\sum_{j \neq h} A_{ij} A_{ih} d_{jh}^{-1}}{k_i(k_i - 1)}.$$

The local efficiency of the entire network is taken as the mean of $E_{\text{loc},i}$ over all nodes in the network.

5. Modularity Q (Newman and Girvan, 2004; Newman, 2004, 2006a): The modularity of a network under a specific partitioning paradigm measures how well the network is divided into non-overlapping groups (or communities) of nodes such that the number of within-group edges is larger than expected in some null model (Newman and Girvan, 2004;

Newman, 2004, 2006a; Porter et al., 2009; Fortunato, 2010). The modularity index is defined as:

$$Q = \sum_{ij} (A_{ij} - \frac{k_i k_j}{2l}) \delta(c_i, c_j),$$

where l is the number of edges in the network, c_i and c_j are the communities containing nodes i and j , respectively, and $\delta(c_i, c_j)$ is the Kronecker delta. In this study, we presented the maximum modularity value obtained with the Louvain algorithm (Blondel et al., 2008) over 100 nearly degenerate solutions (Good et al., 2010).

Acknowledgments. ZZ acknowledges support from the US-China Summer Research Program of the University of Pennsylvania. This work was supported by the John D. and Catherine T. MacArthur Foundation, the Alfred P. Sloan Foundation, the Army Research Laboratory and the Army Research Office through contract numbers W911NF-10-2-0022 and W911NF-14-1-0679, the National Institute of Mental Health (2-R01-DC-009209-11), the National Institute of Child Health and Human Development (1R01HD086888-01), the Office of Naval Research, and the National Science Foundation (BCS-1441502 and BCS-1430087). The funders had no role in study design, data collection and analysis, decision to publish, or preparation of the manuscript. We thank Sarah Feldt Muldoon for helpful comments on an early version of the manuscript.

References

- Abu-Rezq, A. N., Tolba, A. S., Khuwaja, G. A., Foda, S. G., 1999. Best parameters selection for wavelet packet-based compression of magnetic resonance images. *Comput Biomed Res* 32 (5), 449–469.
- Achard, S., Bassett, D. S., Meyer-Lindenberg, A., Bullmore, E., 2008. Fractal connectivity of long-memory networks. *Phys Rev E Stat Nonlin Soft Matter Phys* 77 (3 Pt 2), 036104.
- Achard, S., Bullmore, E., 2007a. Efficiency and cost of economical brain functional networks. *PLoS Comput Biol* 3 (2), e17.
- Achard, S., Bullmore, E., 2007b. Efficiency and cost of economical brain functional networks. *PLoS computational biology* 3 (2), e17.

- Achard, S., Salvador, R., Whitcher, B., Suckling, J., Bullmore, E., 2006a. A resilient, low-frequency, small-world human brain functional network with highly connected association cortical hubs. *J Neurosci* 26 (1), 63–72.
- Achard, S., Salvador, R., Whitcher, B., Suckling, J., Bullmore, E., 2006b. A resilient, low-frequency, small-world human brain functional network with highly connected association cortical hubs. *The Journal of Neuroscience* 26 (1), 63–72.
- Bassett, D. S., Nelson, B. G., Mueller, B. A., Camchong, J., Lim, K. O., 2012. Altered resting state complexity in schizophrenia. *Neuroimage* 59 (3), 2196–2207.
- Bassett, D. S., Porter, M. A., Wymbs, N. F., Grafton, S. T., Carlson, J. M., Mucha, P. J., 2013a. Robust detection of dynamic community structure in networks. *Chaos* 23 (1), 013142.
- Bassett, D. S., Porter, M. A., Wymbs, N. F., Grafton, S. T., Carlson, J. M., Mucha, P. J., 2013b. Robust detection of dynamic community structure in networks. *Chaos: An Interdisciplinary Journal of Nonlinear Science* 23 (1), 013142.
- Bassett, D. S., Wymbs, N. F., Porter, M. A., Mucha, P. J., Carlson, J. M., Grafton, S. T., 2011. Dynamic reconfiguration of human brain networks during learning. *Proc Natl Acad Sci U S A* 108 (18), 7641–7646.
- Bassett, D. S., Wymbs, N. F., Porter, M. A., Mucha, P. J., Grafton, S. T., 2014. Cross-linked structure of network evolution. *Chaos* 24 (1), 013112.
- Bassett, D. S., Wymbs, N. F., Rombach, M. P., Porter, M. A., Mucha, P. J., Grafton, S. T., 2013c. Task-based core-periphery organization of human brain dynamics. *PLoS Comput Biol* 9 (9), e1003171.
- Bassett, D. S., Yang, M., Wymbs, N. F., Grafton, S. T., 2015. Learning-induced autonomy of sensorimotor systems. *arxiv* 1403, 6034.
- Beran, J., 1994. *Statistics for long memory processes*. London: Taylor & Francis.
- Biswal, B., Zerrin Yetkin, F., Haughton, V. M., Hyde, J. S., 1995. Functional connectivity in the motor cortex of resting human brain using echo-planar mri. *Magnetic resonance in medicine* 34 (4), 537–541.

- Blondel, V. D., Guillaume, J.-L., Lambiotte, R., Lefebvre, E., 2008. Fast unfolding of communities in large networks. *Journal of Statistical Mechanics: Theory and Experiment* 2008 (10), P10008.
- Bluhm, R. L., Miller, J., Lanius, R. A., Osuch, E. A., Boksman, K., Neufeld, R., Théberge, J., Schaefer, B., Williamson, P., 2007. Spontaneous low-frequency fluctuations in the bold signal in schizophrenic patients: anomalies in the default network. *Schizophrenia bulletin* 33 (4), 1004–1012.
- Boersma, M., Kemner, C., de Reus, M. A., Collin, G., Snijders, T. M., Hofman, D., Buitelaar, J. K., Stam, C. J., van den Heuvel, M. P., 2013. Disrupted functional brain networks in autistic toddlers. *Brain connectivity* 3 (1), 41–49.
- Breakspear, M., Brammer, M. J., Bullmore, E. T., Das, P., Williams, L. M., 2004. Spatiotemporal wavelet resampling for functional neuroimaging data. *Hum Brain Mapp* 23 (1), 1–25.
- Bullmore, E., Sporns, O., 2012. The economy of brain network organization. *Nat Rev Neurosci* 13 (5), 336–349.
- Bullmore, E. T., Fadili, M. J., Maxim, V., Sendur, L., Whitcher, B., Suckling, J., Brammer, M., Breakspear, M., 2004. Wavelets and functional magnetic resonance imaging of the human brain. *NeuroImage* 23, S234–S249.
- Camchong, J., MacDonald, A. W., Bell, C., Mueller, B. A., Lim, K. O., 2011. Altered functional and anatomical connectivity in schizophrenia. *Schizophrenia bulletin* 37 (3), 640–650.
- Deuker, L., Bullmore, E. T., Smith, M., Christensen, S., Nathan, P. J., Rockstroh, B., Bassett, D. S., 2009. Reproducibility of graph metrics of human brain functional networks. *Neuroimage* 47 (4), 1460–1468.
- Eguiluz, V. M., Chialvo, D. R., Cecchi, G. A., Baliki, M., Apkarian, A. V., 2005. Scale-free brain functional networks. *Physical review letters* 94 (1), 018102.
- Fadili, M. J., Bullmore, E. T., 2004. A comparative evaluation of wavelet-based methods for hypothesis testing of brain activation maps. *Neuroimage* 23 (3), 1112–1128.

- Fornito, A., Bullmore, E. T., 2010. What can spontaneous fluctuations of the blood oxygenation-level-dependent signal tell us about psychiatric disorders? *Current opinion in psychiatry* 23 (3), 239–249.
- Fornito, A., Zalesky, A., Bassett, D. S., Meunier, D., Ellison-Wright, I., Yucel, M., Wood, S. J., Shaw, K., O’Connor, J., Nertney, D., Mowry, B. J., Pantelis, C., Bullmore, E. T., 2011. Genetic influences on cost-efficient organization of human cortical functional networks. *J Neurosci* 31 (9), 3261–3270.
- Fortunato, S., 2010. Community detection in graphs. *Physics Reports* 486, 75–174.
- Freund, Y., Schapire, R., Abe, N., 1999. A short introduction to boosting. *Journal-Japanese Society For Artificial Intelligence* 14 (771-780), 1612.
- Geerligs, L., Maurits, N. M., Renken, R. J., Lorist, M. M., 2014. Reduced specificity of functional connectivity in the aging brain during task performance. *Human brain mapping* 35 (1), 319–330.
- Gencay, R., Selcuk, F., Whitcher, B. J., 2001. An introduction to wavelets and other filtering methods in finance and economics. Academic Press.
- Gießing, C., Thiel, C. M., Alexander-Bloch, A. F., Patel, A. X., Bullmore, E. T., 2013. Human brain functional network changes associated with enhanced and impaired attentional task performance. *The Journal of Neuroscience* 33 (14), 5903–5914.
- Good, B. H., de Montjoye, Y. A., Clauset, A., 2010. Performance of modularity maximization in practical contexts. *Phys Rev E Stat Nonlin Soft Matter Phys* 81 (4 Pt 2), 046106.
- Hagmann, P., Cammoun, L., Gigandet, X., Meuli, R., Honey, C. J., Wedeen, V. J., Sporns, O., 2008. Mapping the structural core of human cerebral cortex. *PLoS biology* 6 (7), e159.
- Honey, C., Sporns, O., Cammoun, L., Gigandet, X., Thiran, J.-P., Meuli, R., Hagmann, P., 2009. Predicting human resting-state functional connectivity from structural connectivity. *Proceedings of the National Academy of Sciences* 106 (6), 2035–2040.

- Honey, C. J., Kötter, R., Breakspear, M., Sporns, O., 2007. Network structure of cerebral cortex shapes functional connectivity on multiple time scales. *Proceedings of the National Academy of Sciences* 104 (24), 10240–10245.
- Humphries, M. D., Gurney, K., 2008. Network small-world-ness: a quantitative method for determining canonical network equivalence. *PloS one* 3 (4), e0002051.
- Hutchison, R. M., Womelsdorf, T., Allen, E. A., Bandettini, P. A., Calhoun, V. D., Corbetta, M., Della Penna, S., Duyn, J. H., Glover, G. H., Gonzalez-Castillo, J., Handwerker, D. A., Keilholz, S., Kiviniemi, V., Leopold, D. A., de Pasquale, F., Sporns, O., Walter, M., Chang, C., 2013. Dynamic functional connectivity: promise, issues, and interpretations. *Neuroimage* 80, 360–378.
- Jakab, A., Emri, M., Spisak, T., Szeman-Nagy, A., Beres, M., Kis, S. A., Molnar, P., Berenyi, E., 2013. Autistic traits in neurotypical adults: correlates of graph theoretical functional network topology and white matter anisotropy patterns. *PLoS One* 8 (4), e60982.
- Lancichinetti, A., Fortunato, S., 2012. Consensus clustering in complex networks. *Scientific reports* 2.
- Latora, V., Marchiori, M., 2001. Efficient behavior of small-world networks. *Physical review letters* 87 (19), 198701.
- Liang, M., Zhou, Y., Jiang, T., Liu, Z., Tian, L., Liu, H., Hao, Y., 2006. Widespread functional disconnectivity in schizophrenia with resting-state functional magnetic resonance imaging. *Neuroreport* 17 (2), 209–213.
- Liu, Y., Liang, M., Zhou, Y., He, Y., Hao, Y., Song, M., Yu, C., Liu, H., Liu, Z., Jiang, T., 2008. Disrupted small-world networks in schizophrenia. *Brain* 131 (4), 945–961.
- Lynall, M. E., Bassett, D. S., Kerwin, R., McKenna, P. J., Kitzbichler, M., Muller, U., Bullmore, E., 2010a. Functional connectivity and brain networks in schizophrenia. *J Neurosci* 30 (28), 9477–9487.

- Lynall, M.-E., Bassett, D. S., Kerwin, R., McKenna, P. J., Kitzbichler, M., Muller, U., Bullmore, E., 2010b. Functional connectivity and brain networks in schizophrenia. *The Journal of Neuroscience* 30 (28), 9477–9487.
- Mantzaris, A. V., Bassett, D. S., Wymbs, N. F., Estrada, E., Porter, M. A., Mucha, P. J., Grafton, S. T., Higham, D. J., 2013. Dynamic network centrality summarizes learning in the human brain. *Journal of Complex Networks* 1 (1), 83–92.
- Maxim, V., Sendur, L., Fadili, M. J., Suckling, J., Gould, R., Howard, R., Bullmore, E., 2005. Fractional gaussian noise, functional MRI and Alzheimer’s disease. *NeuroImage* 25, 141–158.
- Newman, M. E., 2004. Fast algorithm for detecting community structure in networks. *Phys Rev E* 69 (6 Pt 2), 066133.
- Newman, M. E., 2006a. Modularity and community structure in networks. *Proc Natl Acad Sci U S A* 103 (23), 8577–8582.
- Newman, M. E., Girvan, M., 2004. Finding and evaluating community structure in networks. *Physical review E* 69 (2), 026113.
- Newman, M. E. J., 2006b. Modularity and community structure in networks. *Proc. Natl. Acad. Sci. USA* 103, 8577–8582.
- Palit, M., Tudu, B., Dutta, P. K., Dutta, A., Jana, A., Roy, J. K., Bhattacharyya, N., Bandyopadhyay, R., Chatterjee, A., 2010. Classification of black tea taste and correlation with tea taster’s mark using voltammetric electronic tongue. *Instrumentation and Measurement, IEEE Transactions on* 59 (8), 2230–2239.
- Percival, D. B., Walden, A. T., 2000. *Wavelet Methods for Time Series Analysis*. Cambridge University Press.
- Peters, J. M., Taquet, M., Vega, C., Jeste, S. S., Fernandez, I. S., Tan, J., Nelson, C. A. r., Sahin, M., Warfield, S. K., 2013. Brain functional networks in syndromic and non-syndromic autism: a graph theoretical study of EEG connectivity. *BMC Med* 11, 54.
- Porter, M. A., Onnela, J.-P., Mucha, P. J., 2009. Communities in networks. *Notices of the American Mathematical Society* 56 (9), 1082–1097, 1164–1166.

- Pritchard, W. S., Laurienti, P. J., Burdette, J. H., Hayasaka, S., 2014. Functional brain networks formed using cross-sample entropy are scale free. *Brain connectivity* 4 (6), 454–464.
- Quinlan, J. R., 1986. Induction of decision trees. *Machine learning* 1 (1), 81–106.
- Quinlan, J. R., 1993. C4. 5: programs for machine learning. Vol. 1. Morgan kaufmann.
- Schwarz, A. J., McGonigle, J., 2011. Negative edges and soft thresholding in complex network analysis of resting state functional connectivity data. *Neuroimage* 55 (3), 1132–1146.
- Semler, L., Dettori, L., Furst, J., 2005. Wavelet-based texture classification of tissues in computed tomography. In: *Computer-Based Medical Systems, 2005. Proceedings. 18th IEEE Symposium on. IEEE*, pp. 265–270.
- Skudlarski, P., Jagannathan, K., Anderson, K., Stevens, M. C., Calhoun, V. D., Skudlarska, B. A., Pearlson, G., 2010. Brain connectivity is not only lower but different in schizophrenia: a combined anatomical and functional approach. *Biological psychiatry* 68 (1), 61–69.
- Spoormaker, V. I., Schröter, M. S., Gleiser, P. M., Andrade, K. C., Dresler, M., Wehrle, R., Sämann, P. G., Czisch, M., 2010. Development of a large-scale functional brain network during human non-rapid eye movement sleep. *The Journal of neuroscience* 30 (34), 11379–11387.
- Sporns, O., Honey, C. J., Kötter, R., 2007. Identification and classification of hubs in brain networks. *PloS one* 2 (10), e1049.
- Sporns, O., Tononi, G., Edelman, G., 2002. Theoretical neuroanatomy and the connectivity of the cerebral cortex. *Behavioural brain research* 135 (1), 69–74.
- Subasi, A., 2007. Eeg signal classification using wavelet feature extraction and a mixture of expert model. *Expert Systems with Applications* 32 (4), 1084–1093.
- Supekar, K., Menon, V., Rubin, D., Musen, M., Greicius, M. D., 2008. Network analysis of intrinsic functional brain connectivity in alzheimer’s disease. *PLoS computational biology* 4 (6), e1000100.

- Tzourio-Mazoyer, B., Landeau, D., Papathanassiou, F., Crivello, O., Etard, N., Delcroix, B., Joliot, M., 2002a. Automated anatomical labeling of activations in SPM using a macroscopic anatomical parcellation of the MNI MRI single-subject brain. *Neuroimage* 15, 273–289.
- Tzourio-Mazoyer, N., Landeau, B., Papathanassiou, D., Crivello, F., Etard, O., Delcroix, N., Mazoyer, B., Joliot, M., 2002b. Automated anatomical labeling of activations in spm using a macroscopic anatomical parcellation of the mni mri single-subject brain. *Neuroimage* 15 (1), 273–289.
- van den Heuvel, M. P., Stam, C. J., Boersma, M., Hulshoff Pol, H., 2008. Small-world and scale-free organization of voxel-based resting-state functional connectivity in the human brain. *Neuroimage* 43 (3), 528–539.
- Vertes, P. E., Alexander-Bloch, A. F., Gogtay, N., Giedd, J. N., Rapoport, J. L., Bullmore, E. T., 2012. Simple models of human brain functional networks. *Proc Natl Acad Sci U S A* 109 (15), 5868–5873.
- Watts, D., Strogatz, S., 1998. Collective dynamics of 'small-world' networks. *Nature* 393 (6684), 440–442.
- Whitcher, B., Guttorp, P., Percival, D. B., 2000a. Wavelet analysis of covariance with application to atmospheric time series. *J Geophys Res* 105, 941–962.
- Whitcher, B., Guttorp, P., Percival, D. B., 2000b. Wavelet analysis of covariance with application to atmospheric time series. *Journal of Geophysical Research: Atmospheres* (1984–2012) 105 (D11), 14941–14962.
- Wink, A. M., Bernard, F., Salvador, R., Bullmore, E. T., Suckling, J., 2006. Age and cholinergic effects on hemodynamics and functional coherence of human hippocampus. *Neurobiol Aging* 27, 1395–1404.
- Zalesky, A., Fornito, A., Bullmore, E., 2012. On the use of correlation as a measure of network connectivity. *Neuroimage* 60 (4), 2096–2106.

Supplementary Material for “Choosing Wavelet Methods, Filters, and Lengths for Functional Brain Network Construction”

Zitong Zhang^{a,b}, Qawi K. Telesford^b, Chad Giusti^{b,c}, Kelvin O. Lim^d,
Danielle S. Bassett^{b,e}

^a*Department of Biomedical Engineering, Tsinghua University, Beijing 100084, China*

^b*Department of Bioengineering, University of Pennsylvania, Philadelphia, PA 19104, USA*

^c*Warren Center for Network and Data Sciences, University of Pennsylvania, PA 19104, USA*

^d*Department of Psychiatry, University of Minnesota, Minneapolis, MN 55455, USA*

^e*Department of Electrical and Systems Engineering, University of Pennsylvania, Philadelphia, PA 19104, USA*

Keywords: Wavelet Filters, Functional brain network, fMRI, Network diagnostics

1. Supplemental Methods

1.1. Wavelet Coefficients and Wavelet Details

The j th level MODWT wavelet and scaling coefficients for signal \mathbf{X} with length N are defined, respectively, as:

$$\tilde{W}_{j,t} = \sum_{l=0}^{L_j-1} \tilde{h}_{j,l} X_{t-l \bmod N} \text{ and } \tilde{Y}_{j,t} = \sum_{l=0}^{L_j-1} \tilde{g}_{j,l} X_{t-l \bmod N},$$

where $\{\tilde{h}_{j,l}\}$ and $\{\tilde{g}_{j,l}\}$ are the j th level MODWT wavelet and scaling filters, and L_j is their common length. In matrix form, the above expression can also be written as:

$$\tilde{\mathbf{W}}_j = \tilde{W}_j \mathbf{X} \text{ and } \tilde{\mathbf{Y}}_j = \tilde{Y}_j \mathbf{X}.$$

Together, the wavelet and scaling coefficients form an energy decomposition and ANOVA of the original signal:

$$\|\mathbf{X}\|^2 = \sum_{j=1}^{J_0} \|\tilde{\mathbf{W}}_j\|^2 + \|\tilde{\mathbf{Y}}_{J_0}\|^2.$$

On the other hand, the j th level details and smooths are defined by:

$$\tilde{D}_j = \tilde{W}_j^T \tilde{\mathbf{W}}_j \text{ and } \tilde{S}_j = \tilde{Y}_j^T \tilde{\mathbf{Y}}_j.$$

Together, they define a multiresolution analysis (MRA) of the signal:

$$\mathbf{X} = \sum_{j=1}^{J_0} \tilde{D}_j + \tilde{S}_{J_0}.$$

1.2. Wavelet Coherence

The wavelet coherence of two signals x and y is defined as (Grinsted et al., 2004):

$$G[Cx^*(a, b)Cy(a, b)] / [\sqrt{G(|Cx(a, b)|^2)} \sqrt{G(|Cy(a, b)|^2)}],$$

where $Cx(a, b)$ and $Cy(a, b)$ represent the continuous wavelet transform (CWT) of x and y , respectively, and G stands for a smoothing operator in time and scale. In this study, we have averaged 10 adjacent time points and have not smoothed in scale. Note that scale 1~4 correspond to $a = 1, 2, 4$, and 8 , respectively. To calculate the value of connectivity between two brain regions, we then compute the average of this time course.

2. Supplemental Results

2.1. Network Diagnostic Values Across Frequency Bands

In the main manuscript, we report network diagnostic values obtained from functional brain networks constructed from scale 2 wavelet coefficients. In particular, we report that wavelet filter type (D, LA, and C) has little effect on estimated diagnostics for identical wavelet lengths. Here we show similar results for functional brain networks constructed from scale 1 (approximately 0.125–0.25 Hz; see Fig. 1), scale 3 (approximately 0.03–0.06 Hz; see Fig. 2), and scale 4 (approximately 0.015–0.03 Hz; see Fig. 3) wavelet coefficients.

2.2. Network Diagnostic Values Across Densities

In the main manuscript, we report network diagnostic values obtained from functional brain networks constructed from the 30% strongest connections. Here we show similar results for functional brain networks constructed from the 25% strongest connections (see Fig. 4) and the 35% strongest connections (see Fig. 5). These results are both quantitatively and qualitatively similar to those reported for networks constructed from the 30% strongest connections, suggesting that our conclusion regarding these data (namely that wavelet filter type – D, LA, and C – has little effect on estimated diagnostics for identical wavelet lengths) is robust to small variations in network density.

2.3. Frequency Dependence of Wavelet Filter Length Effects

In the main manuscript, we observe that the length of the wavelet filter differentially effects network diagnostics obtained from functional brain networks constructed from scale 2 wavelet coefficients; some diagnostics are affected significantly (such as the modularity index), and other diagnostics are affected very little (such as the characteristic path length). We quantify this differential sensitivity using a set of repeated measures ANOVA (ANalysis Of VAriance), for each diagnostic and each type of wavelet filter, where wavelet length was treated as a categorical factor, and diagnostic type was treated as a repeated measure.

Here we ask whether this differential sensitivity is dependent on frequency by performing the same set of ANOVAs for functional brain networks constructed from scale 1 (Tab. 1), scale 3 (Tab. 2), and scale 4 (Tab. 3) wavelet coefficients. The pattern of results in the functional brain networks constructed from scale 1 wavelet coefficients is very consistent with that observed

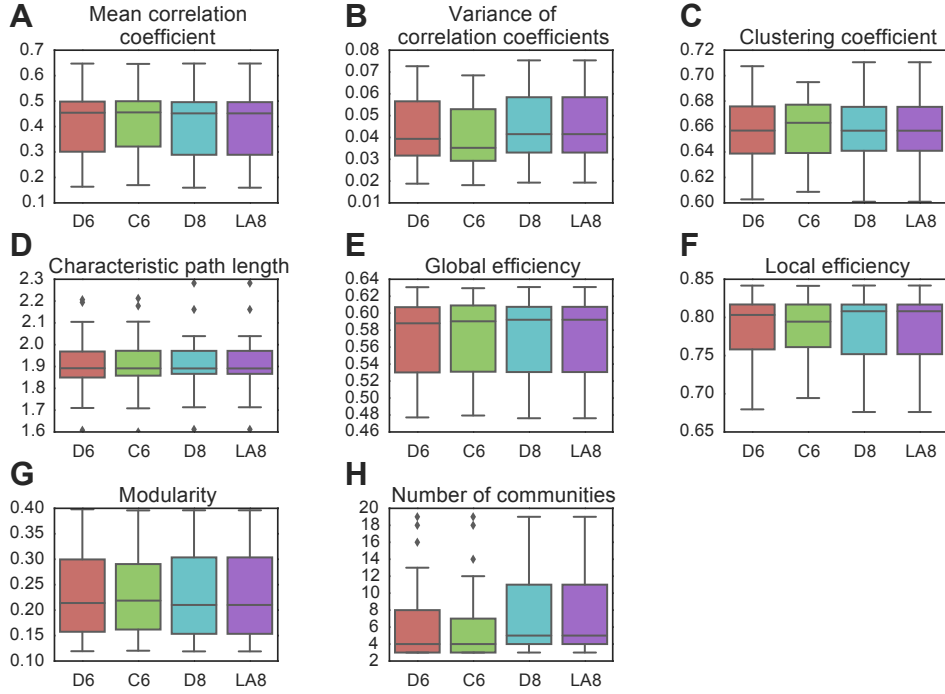


Figure 1: **Effect of Wavelet Filter on Network Diagnostics** in wavelet scale 1 between pairs of wavelet filters with the same length. (A, B) Weighted network diagnostics including (A) mean correlation coefficient and (B) variance of correlation coefficients. (C–F) Binary network diagnostics calculated at a graph density of 30% obtained through a cumulative thresholding procedure, including (C) the clustering coefficient, (D) characteristic path length, (E) global efficiency, (F) local efficiency, (G) modularity index Q , and (H) the number of communities. Boxplots indicate the median and quartiles of the data acquired from 29 health subjects.

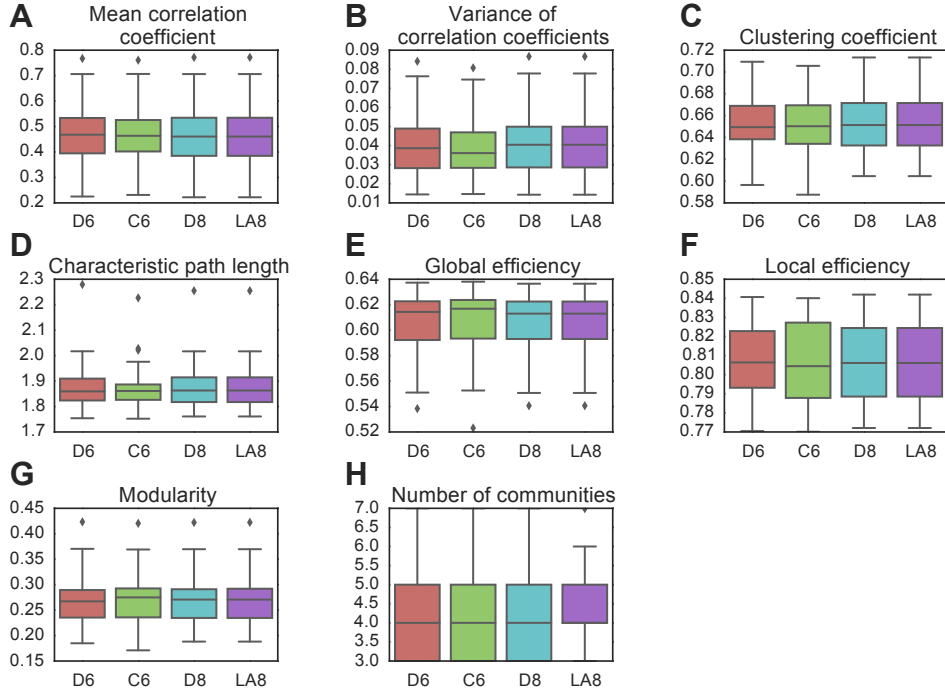


Figure 2: **Effect of Wavelet Filter on Network Diagnostics** in wavelet scale 3 between pairs of wavelet filters with the same length. (A, B) Weighted network diagnostics including (A) mean correlation coefficient and (B) variance of correlation coefficients. (C–F) Binary network diagnostics calculated at a graph density of 30% obtained through a cumulative thresholding procedure, including (C) the clustering coefficient, (D) characteristic path length, (E) global efficiency, (F) local efficiency, (G) modularity index Q , and (H) the number of communities. Boxplots indicate the median and quartiles of the data acquired from 29 health subjects.

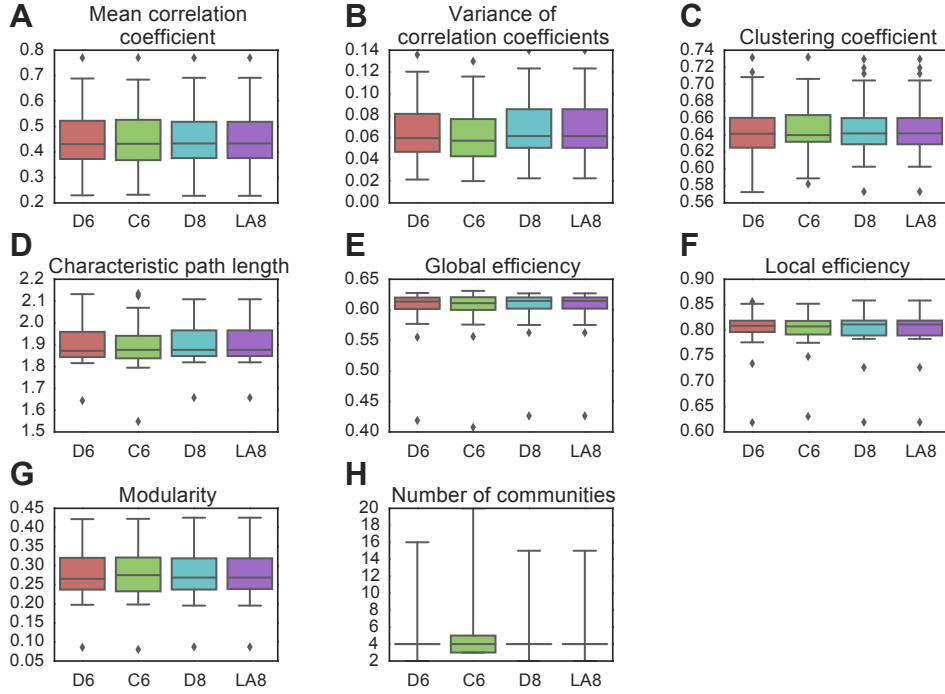


Figure 3: **Effect of Wavelet Filter on Network Diagnostics** in wavelet scale 4 between pairs of wavelet filters with the same length. (A, B) Weighted network diagnostics including (A) mean correlation coefficient and (B) variance of correlation coefficients. (C–F) Binary network diagnostics calculated at a graph density of 30% obtained through a cumulative thresholding procedure, including (C) the clustering coefficient, (D) characteristic path length, (E) global efficiency, (F) local efficiency, (G) modularity index Q , and (H) the number of communities. Boxplots indicate the median and quartiles of the data acquired from 29 health subjects.

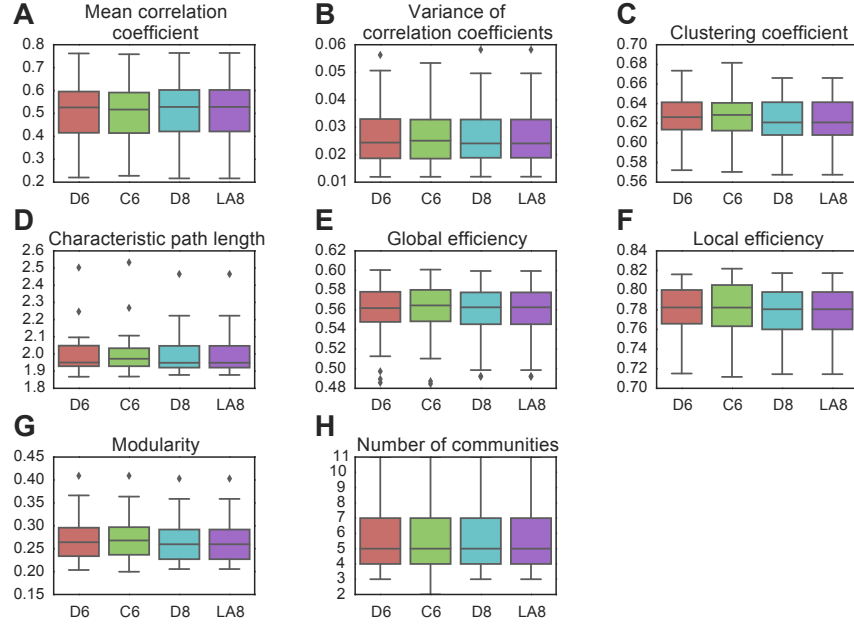


Figure 4: **Effect of Wavelet Filter on Network Diagnostics** in wavelet scale 2 between pairs of wavelet filters with the same length. (A, B) Weighted network diagnostics including (A) mean correlation coefficient and (B) variance of correlation coefficients. (C–F) Binary network diagnostics calculated at a graph density of 25% obtained through a cumulative thresholding procedure, including (C) the clustering coefficient, (D) characteristic path length, (E) global efficiency, (F) local efficiency, (G) modularity index Q , and (H) the number of communities. Boxplots indicate the median and quartiles of the data acquired from 29 health subjects.

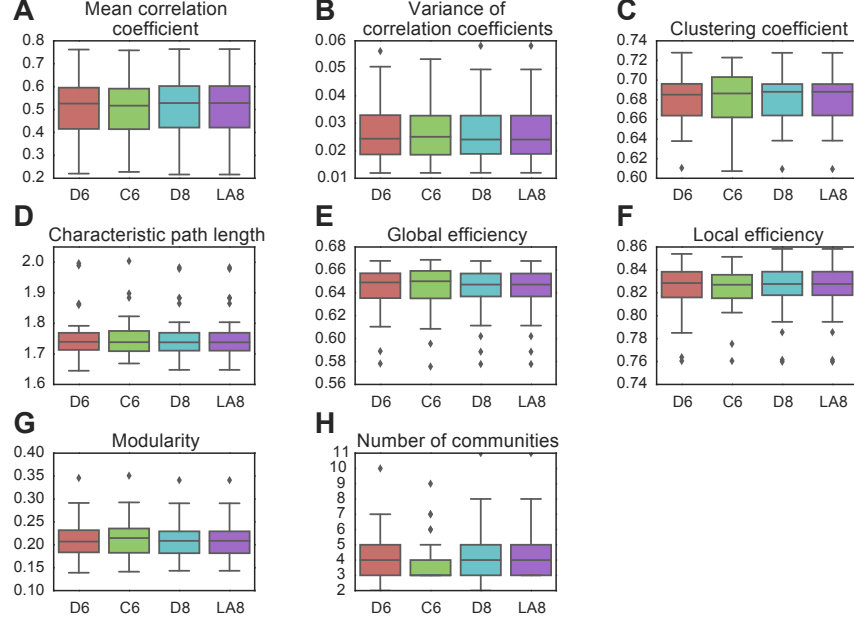


Figure 5: **Effect of Wavelet Filter on Network Diagnostics** in wavelet scale 2 between pairs of wavelet filters with the same length. (A, B) Weighted network diagnostics including (A) mean correlation coefficient and (B) variance of correlation coefficients. (C–F) Binary network diagnostics calculated at a graph density of 35% obtained through a cumulative thresholding procedure, including (C) the clustering coefficient, (D) characteristic path length, (E) global efficiency, (F) local efficiency, (G) modularity index Q , and (H) the number of communities. Boxplots indicate the median and quartiles of the data acquired from 29 health subjects.

for functional brain networks constructed from scale 2 wavelet coefficients (compare Tab. 1 in this supplement with Tab. 2 in the main manuscript). In both cases, the mean correlation coefficient, variance of the correlation coefficients, and number of communities tend to be sensitive to wavelet length across all wavelet filter types (D, LA, and C). Observed effects in global efficiency, local efficiency, and modularity are less consistent across the two frequency bands.

Interestingly, in functional brain networks constructed from scale 3 wavelet coefficients, we observe that only one network diagnostic shows a significant wavelet length effect, and that is the variance of the correlation coefficients. In functional brain networks constructed from scale 4 wavelet coefficients,

we observe robust main effects of wavelet length on the mean correlation coefficient, the variance of the correlation coefficients, and the modularity index.

In summary, the variance of the correlation coefficients is affected by wavelet length across all three wavelet types (D, LA, and C), and across all frequency bands examined (associated with scale 1, 2, 3, and 4 wavelet coefficients). Other network diagnostics showed differential sensitivity to wavelet length in the 4 frequency bands.

2.4. Frequency Dependence of Assessed Group Differences

In the main manuscript, we present a set of analyses to assess group differences between healthy controls and schizophrenia patients in network diagnostic values obtained from functional brain networks constructed from scale 2 wavelet coefficients, corresponding approximately to the frequency range 0.06–0.12 Hz. We observed that group differences were most salient at longer wavelet lengths, across the 3 filter types, and especially for the following network diagnostics: mean correlation coefficient, variance of correlation coefficients, clustering coefficient, modularity, and number of communities.

Here, we ask whether these results are frequency dependent by assessing group differences in network diagnostic values obtained from functional brain networks constructed from scale 1 (approximately 0.125–0.25 Hz; see Fig. 6), scale 3 (approximately 0.03–0.06 Hz; see Fig. 7), and scale 4 (approximately 0.015–0.03 Hz; see Fig. 8) wavelet coefficients. Visually, we observe that group differences are more salient at smaller wavelet lengths than larger wavelet lengths in functional brain networks constructed from scale 1 coefficients, especially for the mean correlation coefficient, variance in correlation coefficients, local efficiency, and number of communities. Group differences are much weaker over all (for both long and short wavelets) in functional brain networks extracted from scale 3 and scale 4 coefficients, corresponding to BOLD signal variation in lower frequency bands (< 0.06 Hz).

Together, these results indicate that (i) group differences in functional brain network architecture can be differentially salient across frequency bands, and that (ii) the optimal wavelet filter length may depend upon the frequency band of interest. In this dataset, we observe that longer wavelets are more sensitive to group differences in functional brain networks constructed from wavelet scale 2 coefficients, whose smoothness might facilitate a more sensitive characterization of low frequency fluctuations in the BOLD signal. In contrast, shorter wavelets are more sensitive to group differences in functional

	Daubechies Extremal Phase (dF=9,252)		Daubechies Least Asymmetric (dF=6,168)		Coiflet (dF=3,84)	
	F	p	F	p	F	p
Mean correlation coefficient	27.97	0.0000	29.34	0.0000	32.31	0.0000
Variance of correlation coefficients	94.97	0.0000	102.80	0.0000	103.99	0.0000
Clustering coefficient	0.17	0.9966	0.50	0.8068	0.22	0.8820
Characteristic path length	0.15	0.9978	0.13	0.9923	0.46	0.7082
Global efficiency	8.60	0.0000	1.75	0.1129	4.52	0.0055
Local efficiency	2.01	0.0389	0.58	0.7451	1.77	0.1582
Modularity	0.39	0.9410	0.51	0.7976	0.11	0.9513
Number of communities	4.87	0.0000	2.18	0.0476	4.81	0.0039

Table 1: **Effect of Wavelet Length.** Results of Repeated Measures ANOVAs for network diagnostics extracted from 29 healthy controls at scale 1 and a graph density of 30%; network diagnostic is treated as a factor and wavelet length is treated as a repeated measure, separately for each wavelet filter type. Effects that are significant at $p < 0.05$, uncorrected, are shown in red.

	Daubechies Extremal Phase (dF=9,252)		Daubechies Least Asymmetric (dF=6,168)		Coiflet (dF=3,84)	
	<i>F</i>	<i>p</i>	<i>F</i>	<i>p</i>	<i>F</i>	<i>p</i>
Mean	0.58	0.8126	0.77	0.5963	0.87	0.4591
correlation coefficient						
Variance of	34.05	0.0000	52.72	0.0000	44.25	0.0000
correlation coefficients						
Clustering coefficient	0.36	0.9512	0.37	0.8950	0.20	0.8995
Characteristic path length	0.67	0.7331	1.78	0.1061	0.73	0.5383
Global efficiency	0.82	0.5966	1.32	0.2522	1.06	0.3709
Local efficiency	0.67	0.7332	0.45	0.8424	0.23	0.8782
Modularity	0.21	0.9932	0.95	0.4588	0.24	0.8711
Number of communities	0.65	0.7555	1.21	0.3019	0.22	0.8806

Table 2: **Effect of Wavelet Length.** Results of Repeated Measures ANOVAs for network diagnostics extracted from 29 healthy controls at scale 3 and a graph density of 30%; network diagnostic is treated as a factor and wavelet length is treated as a repeated measure, separately for each wavelet filter type. Effects that are significant at $p < 0.05$, uncorrected, are shown in red.

	Daubechies Extremal Phase (dF=9,252)		Daubechies Least Asymmetric (dF=6,168)		Coiflet (dF=3,84)	
	<i>F</i>	<i>p</i>	<i>F</i>	<i>p</i>	<i>F</i>	<i>p</i>
Mean	4.81	0.0000	7.52	0.0000	5.65	0.0014
correlation coefficient						
Variance of	92.21	0.0000	106.66	0.0000	105.99	0.0000
correlation coefficients						
Clustering coefficient	1.64	0.1052	0.84	0.5396	0.33	0.8037
Characteristic path length	0.35	0.9571	0.58	0.7495	0.65	0.5839
Global efficiency	0.19	0.9948	1.12	0.3514	0.58	0.6276
Local efficiency	1.01	0.4310	0.54	0.7781	0.29	0.8302
Modularity	5.30	0.0000	5.76	0.0000	4.27	0.0074
Number of communities	0.86	0.5587	1.11	0.3607	2.20	0.0941

Table 3: **Effect of Wavelet Length.** Results of Repeated Measures ANOVAs for network diagnostics extracted from 29 healthy controls at scale 4 and a graph density of 30%; network diagnostic is treated as a factor and wavelet length is treated as a repeated measure, separately for each wavelet filter type. Effects that are significant at $p < 0.05$, uncorrected, are shown in red.

brain networks constructed from wavelet scale 1 coefficients, whose discrete nature might facilitate a more sensitive characterization of high frequency fluctuations in the BOLD signal.

2.5. Dependence of Assessed Group Differences on Methodological Choices

In the main manuscript, we observed that the p -values for parametric t -tests measuring differences in network diagnostic values between healthy controls and people with schizophrenia decreased with increasing wavelet length, suggesting that longer wavelets display greater statistical sensitivity to group differences in these data. Here in the SI, we explore the dependence of these results on methodological choices in network construction.

1. First, we examine the effect of the frequency band of interest. In the main manuscript, we assess functional brain networks constructed from scale 2 wavelet coefficients, and demonstrate that group differences in network diagnostics are most salient at longer wavelet lengths. Here we show that group differences in network diagnostics extracted from functional brain networks constructed from scale 1 wavelet coefficients are more salient at short wavelet lengths (see Fig. 9). Therefore, group differences are differentially assessed across frequency bands.
2. Second, we examine the effect of the measure of functional connectivity, including partial correlation (Fig. 10 and 11), wavelet coherence (see Supplemental Methods; Fig. 12 and 13), and wavelet correlation (see main manuscript). We observe that the effect of wavelet length is more salient when using wavelet correlation than when using wavelet coherence or partial correlation.
3. Third, we examine the effect of the strength of edges. In the main manuscript, we examined networks constructed from the 30% strongest connections. Here, we ask whether networks constructed from weak connections might provide complementary information, as recently proposed in the literature (Bassett et al., 2012; Schwarz and McGonigle, 2011). Specifically, we examine group differences in network diagnostics extracted from functional brain networks constructed from the 30% weakest (see Fig. 14 and 15), 10% weakest (Fig. 16 and 17), and 1% weakest (Fig. 18 and 19) connections, where connectivity is defined as the wavelet correlation between scale 1 or 2 wavelet coefficients. We observe that the effect of wavelet length is more salient when using the strongest 30% connections or 10% weakest connections than when using the 30% or 1% weakest connections.

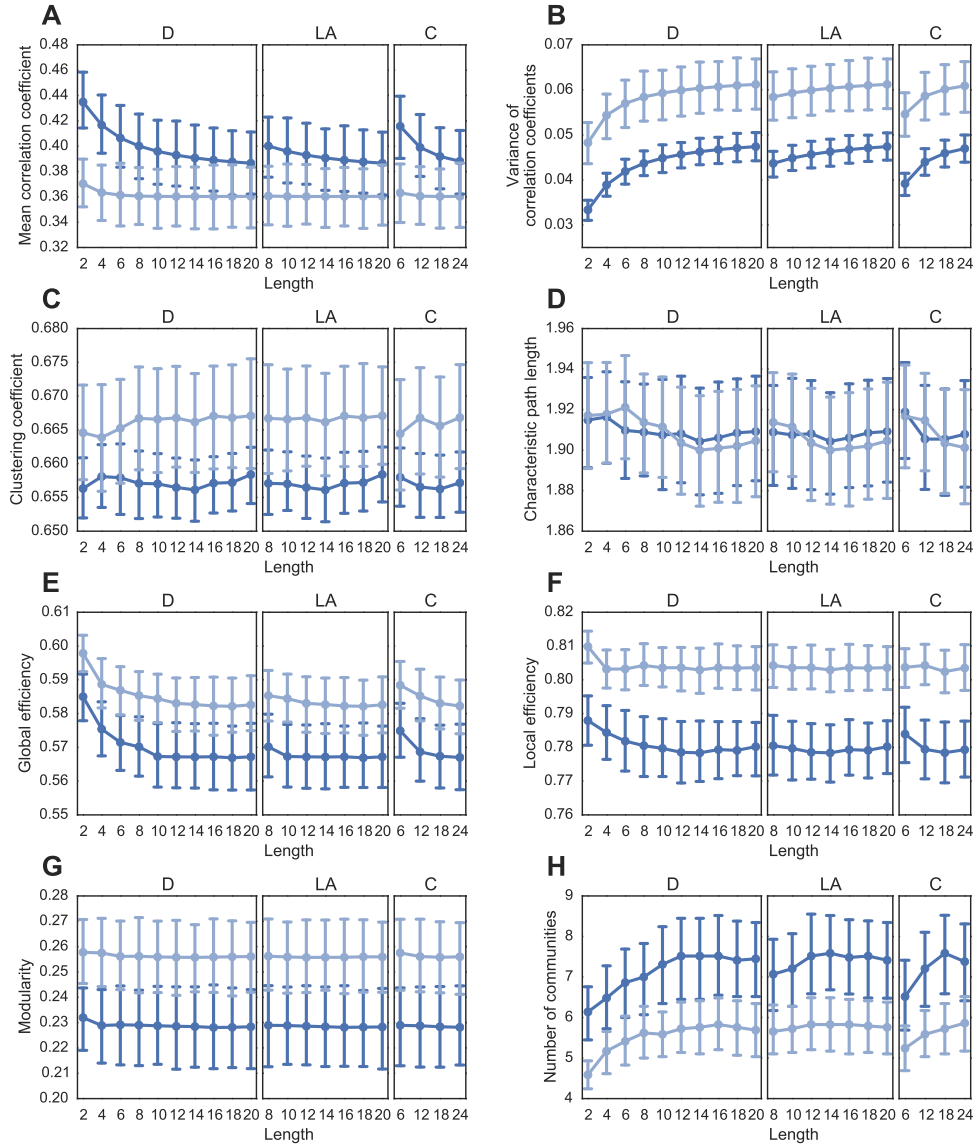


Figure 6: **Effect of Wavelet Length on Network Diagnostics** in wavelet scale 1 for all wavelet filters. (A, B) Weighted network diagnostics including (A) mean correlation coefficient and (B) variance of correlation coefficients. (C-F) Binary network diagnostics calculated at a graph density of 30% obtained through a cumulative thresholding procedure, including (C) the clustering coefficient, (D) characteristic path length, (E) global efficiency, (F) local efficiency, (G) modularity index Q , and (H) the number of communities. The more saturated curves represent data from the 29 healthy controls, while the less saturated curves represent data from 29 people with schizophrenia. Error bars depict standard errors of the mean across subjects.

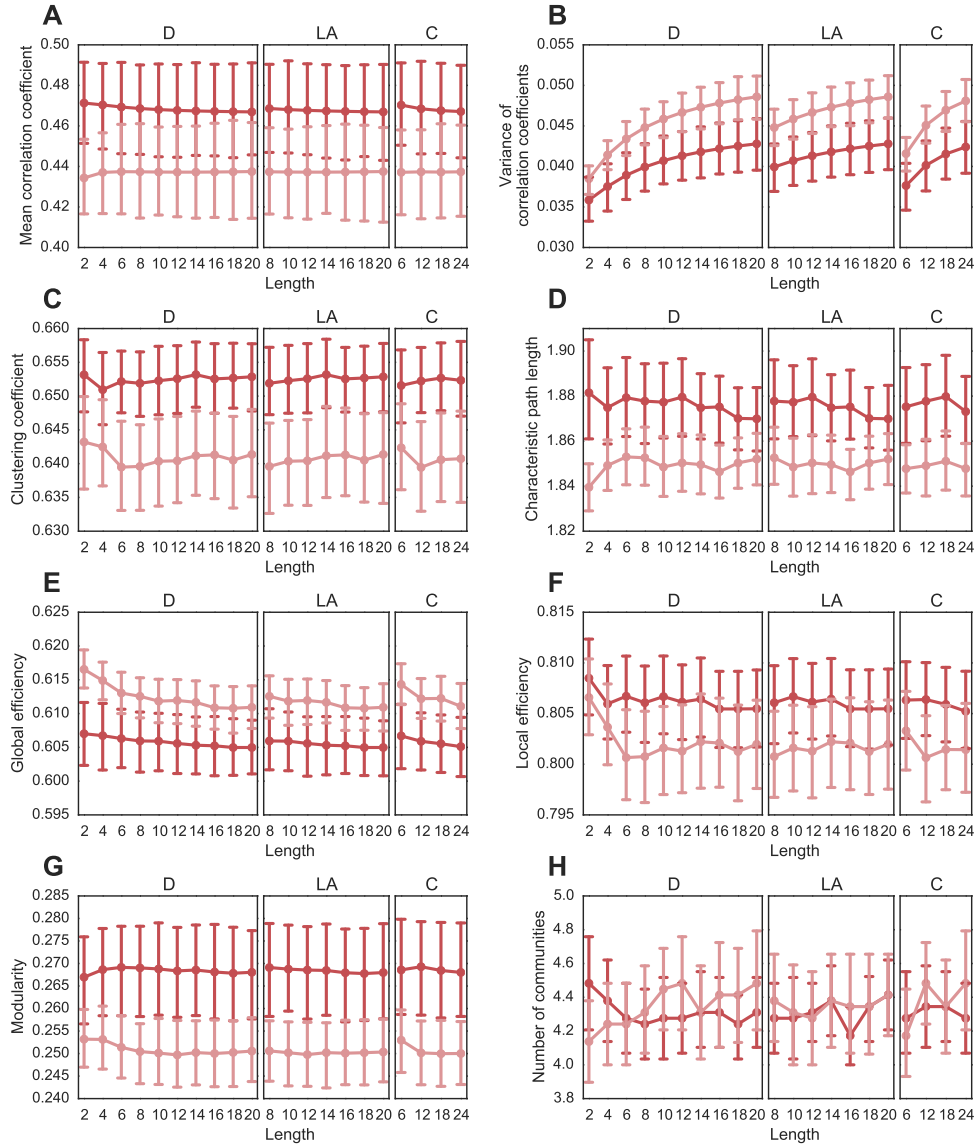


Figure 7: **Effect of Wavelet Length on Network Diagnostics** in wavelet scale 3 for all wavelet filters. (A, B) Weighted network diagnostics including (A) mean correlation coefficient and (B) variance of correlation coefficients. (C-F) Binary network diagnostics calculated at a graph density of 30% obtained through a cumulative thresholding procedure, including (C) the clustering coefficient, (D) characteristic path length, (E) global efficiency, (F) local efficiency, (G) modularity index Q , and (H) the number of communities. The more saturated curves represent data from the 29 healthy controls, while the less saturated curves represent data from 29 people with schizophrenia. Error bars depict standard errors of the mean across subjects.

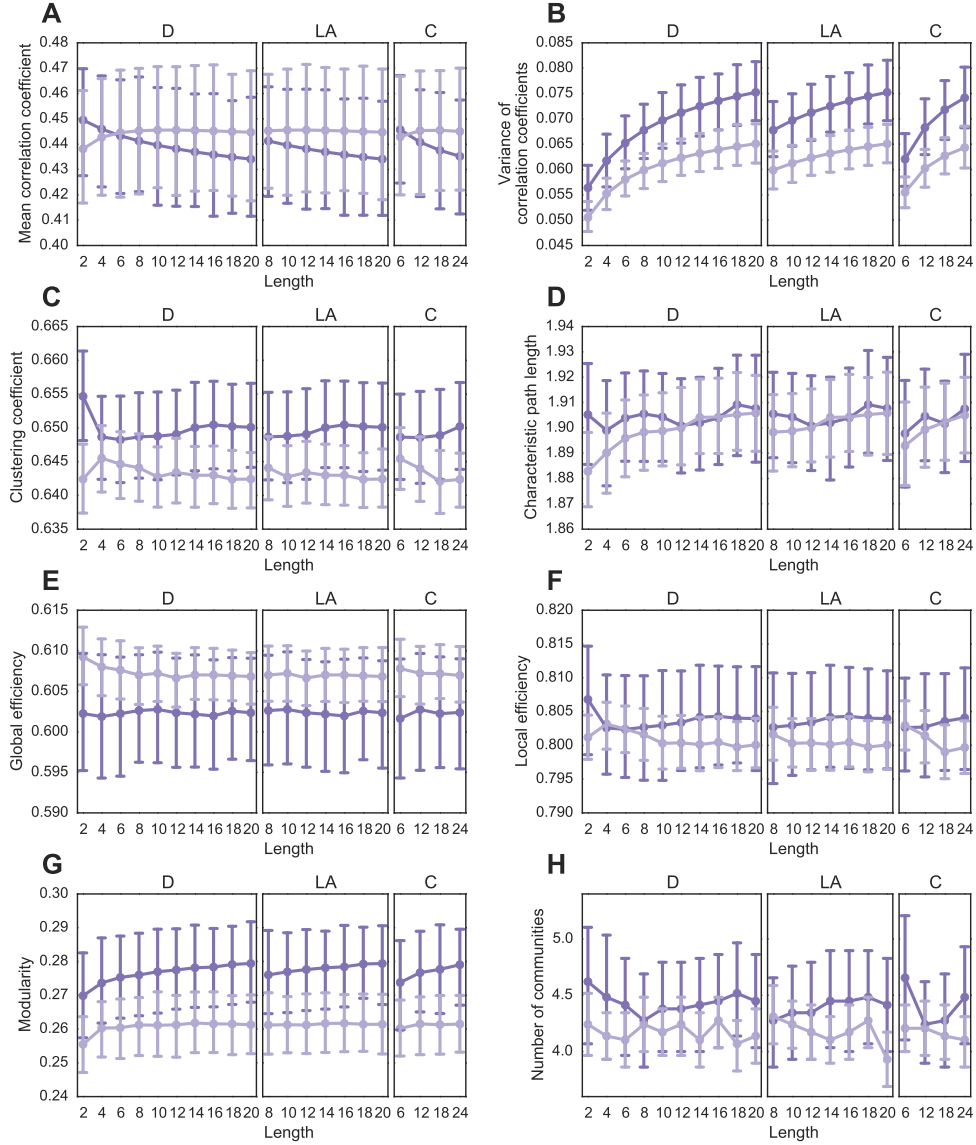


Figure 8: **Effect of Wavelet Length on Network Diagnostics** in wavelet scale 4 for all wavelet filters. (A, B) Weighted network diagnostics including (A) mean correlation coefficient and (B) variance of correlation coefficients. (C–F) Binary network diagnostics calculated at a graph density of 30% obtained through a cumulative thresholding procedure, including (C) the clustering coefficient, (D) characteristic path length, (E) global efficiency, (F) local efficiency, (G) modular index Q , and (H) the number of communities. The more saturated curves represent data from the 29 healthy controls, while the less saturated curves represent data from 29 people with schizophrenia. Error bars depict standard errors of the mean across subjects.

4. Fourth, we examine the effect of choosing wavelet details (see Supplemental Methods) over wavelet coefficients (see Fig. 20 and 21). Results are consistent across the use of both wavelet details and wavelet coefficients.

In summary, we observe that the impact of wavelet length on group differences is (i) dependent on frequency, (ii) more salient when using wavelet correlation than when using wavelet coherence or partial correlation, (iii) more salient when using the strongest 30% connections or 10% weakest connections than when using the 30% or 1% weakest connections, and (iv) relatively agnostic to the use of either wavelet details or wavelet coefficients.

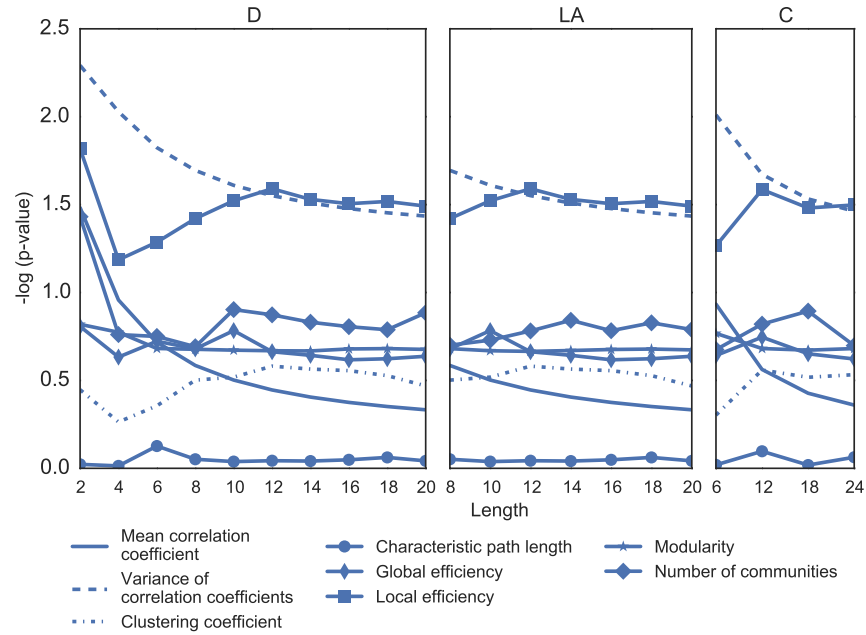


Figure 9: Effect of Wavelet Filter Type and Length on Statistical Sensitivity in Group Comparisons. Negative common logarithm of the p -values obtained from two-sample t -tests between diagnostic values extracted from healthy control networks versus those extracted from schizophrenia patient networks. Network diagnostics are calculated for functional brain networks constructed from scale 1 wavelet coefficients. Networks represent the strongest 30% of edges.

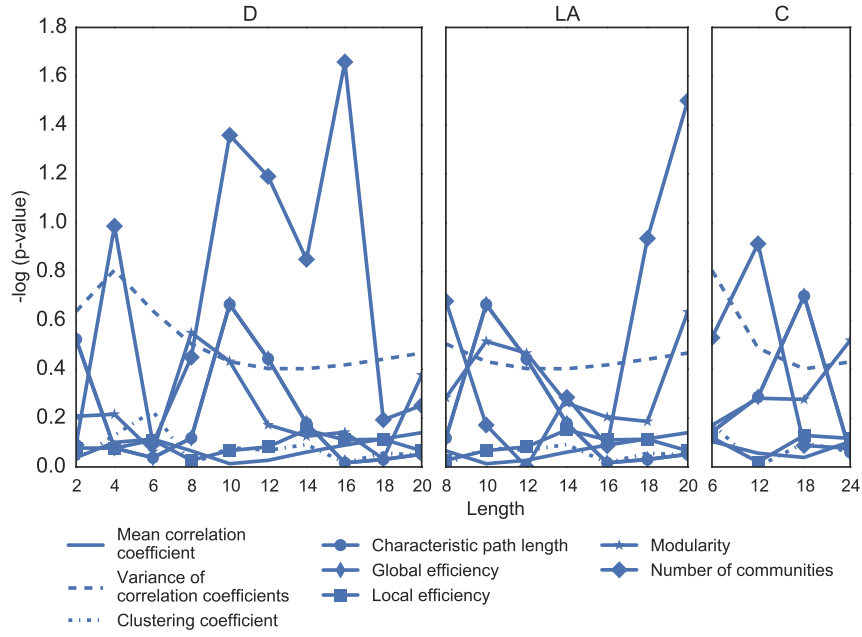


Figure 10: Effect of Wavelet Filter Type and Length on Statistical Sensitivity in Group Comparisons. Negative common logarithm of the p -values obtained from two-sample t -tests between diagnostic values extracted from healthy control networks versus those extracted from schizophrenia patient networks. Network diagnostics are calculated for functional brain networks constructed from scale 1 wavelet coefficients. Networks represent the strongest 30% of edges, and functional connectivity is calculated from partial correlations in wavelet coefficients.

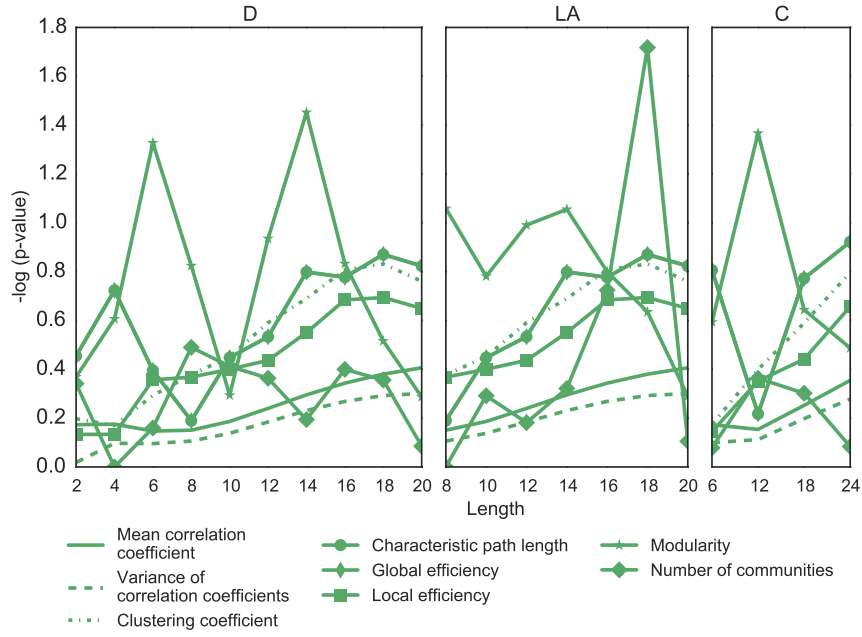


Figure 11: Effect of Wavelet Filter Type and Length on Statistical Sensitivity in Group Comparisons. Negative common logarithm of the p -values obtained from two-sample t -tests between diagnostic values extracted from healthy control networks versus those extracted from schizophrenia patient networks. Network diagnostics are calculated for functional brain networks constructed from scale 2 wavelet coefficients. Networks represent the strongest 30% of edges, and functional connectivity is calculated from partial correlations in wavelet coefficients.

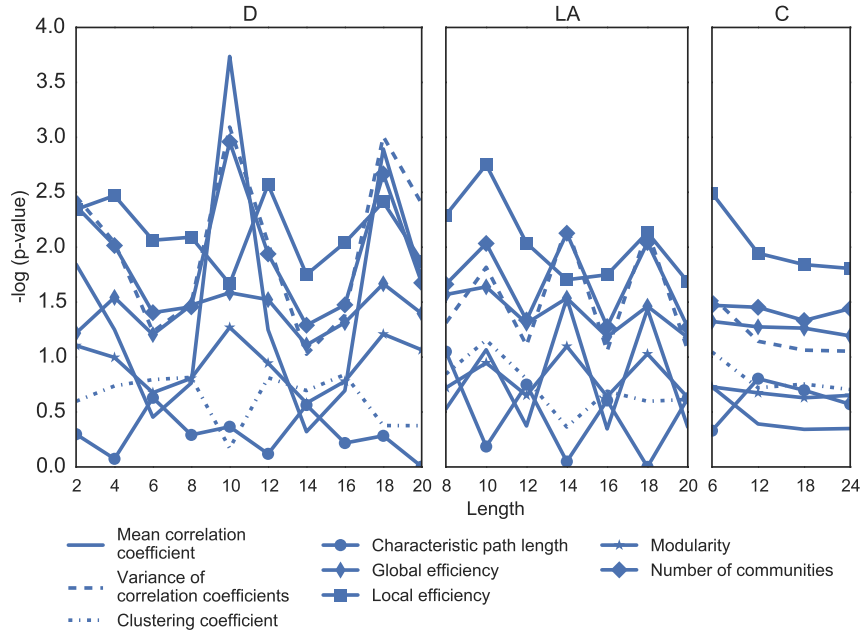


Figure 12: Effect of Wavelet Filter Type and Length on Statistical Sensitivity in Group Comparisons. Negative common logarithm of the p -values obtained from two-sample t -tests between diagnostic values extracted from healthy control networks versus those extracted from schizophrenia patient networks. Network diagnostics are calculated for functional brain networks constructed from scale 1 wavelet coefficients. Networks represent the strongest 30% of edges, and functional connectivity is calculated from wavelet coherence.

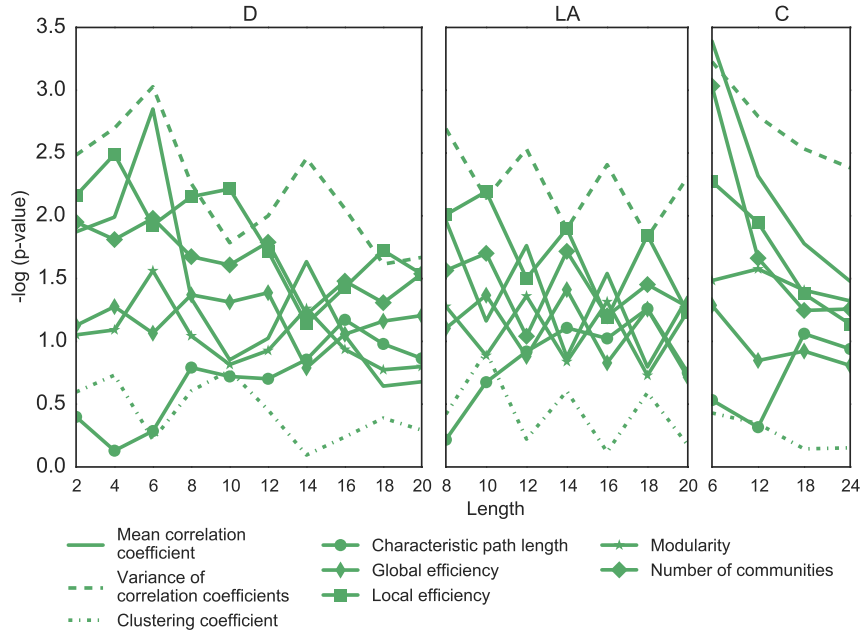


Figure 13: Effect of Wavelet Filter Type and Length on Statistical Sensitivity in Group Comparisons. Negative common logarithm of the p -values obtained from two-sample t -tests between diagnostic values extracted from healthy control networks versus those extracted from schizophrenia patient networks. Network diagnostics are calculated for functional brain networks constructed from scale 2 wavelet coefficients. Networks represent the strongest 30% of edges, and functional connectivity is calculated from wavelet coherence.

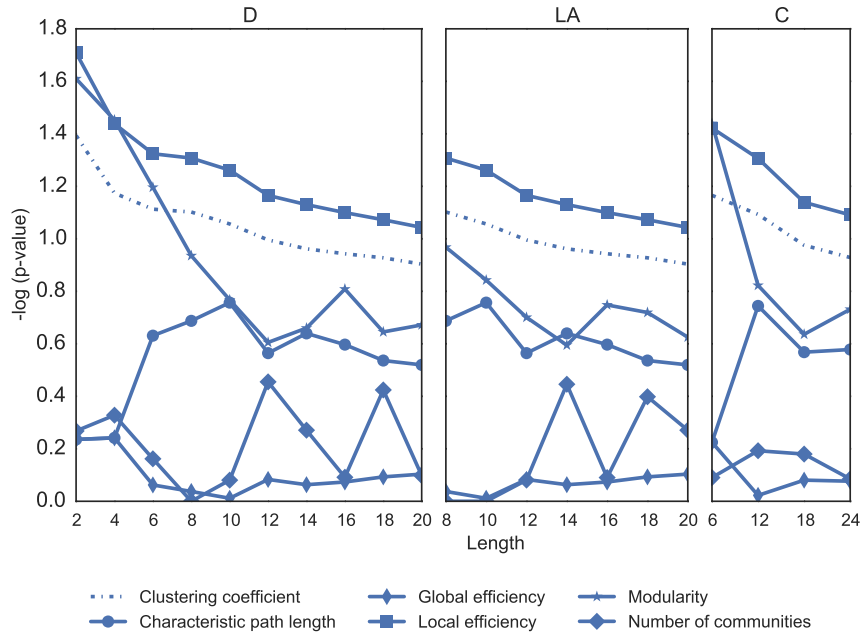


Figure 14: Effect of Wavelet Filter Type and Length on Statistical Sensitivity in Group Comparisons. Negative common logarithm of the p -values obtained from two-sample t -tests between diagnostic values extracted from healthy control networks versus those extracted from schizophrenia patient networks. Network diagnostics are calculated for functional brain networks constructed from scale 1 wavelet coefficients. Networks represent the weakest 30% of edges.

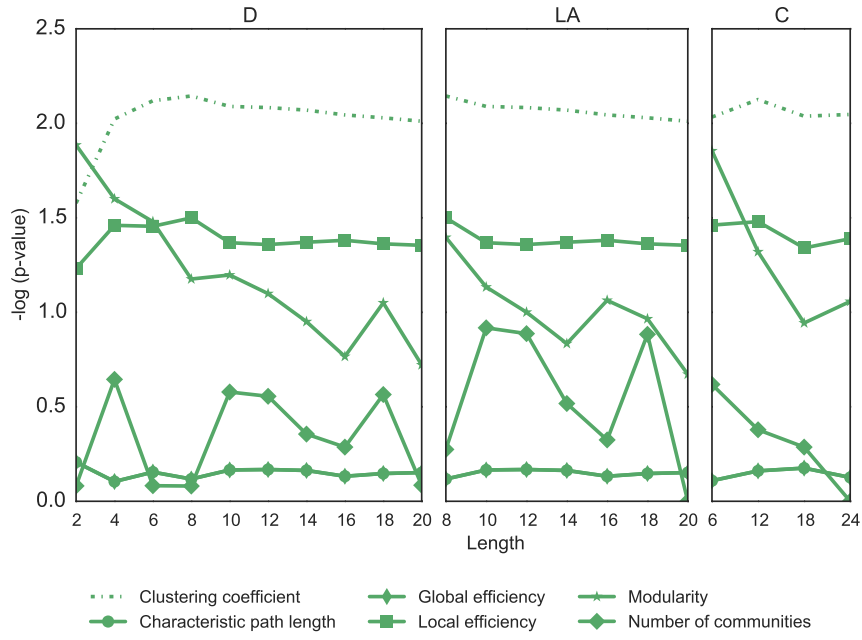


Figure 15: **Effect of Wavelet Filter Type and Length on Statistical Sensitivity in Group Comparisons.** Negative common logarithm of the p -values obtained from two-sample t -tests between diagnostic values extracted from healthy control networks versus those extracted from schizophrenia patient networks. Network diagnostics are calculated for functional brain networks constructed from scale 2 wavelet coefficients. Networks represent the weakest 30% of edges.

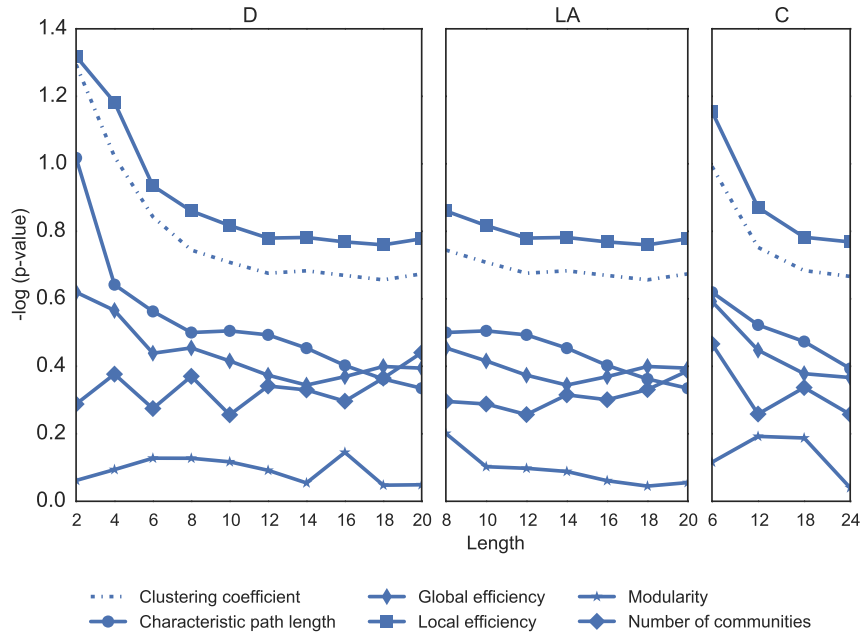


Figure 16: Effect of Wavelet Filter Type and Length on Statistical Sensitivity in Group Comparisons. Negative common logarithm of the p -values obtained from two-sample t -tests between diagnostic values extracted from healthy control networks versus those extracted from schizophrenia patient networks. Network diagnostics are calculated for functional brain networks constructed from scale 1 wavelet coefficients. Networks represent the weakest 10% of edges.

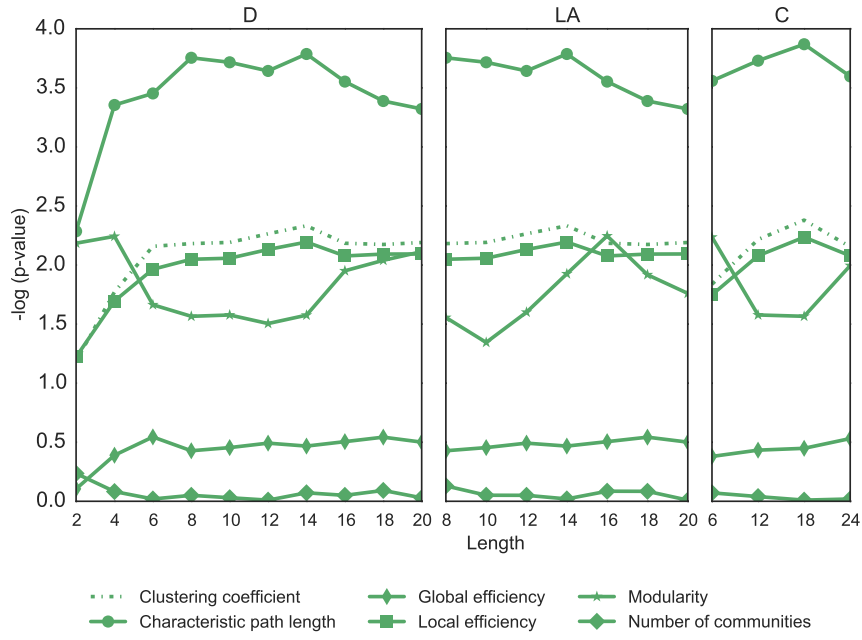


Figure 17: **Effect of Wavelet Filter Type and Length on Statistical Sensitivity in Group Comparisons.** Negative common logarithm of the p -values obtained from two-sample t -tests between diagnostic values extracted from healthy control networks versus those extracted from schizophrenia patient networks. Network diagnostics are calculated for functional brain networks constructed from scale 2 wavelet coefficients. Networks represent the weakest 10% of edges.

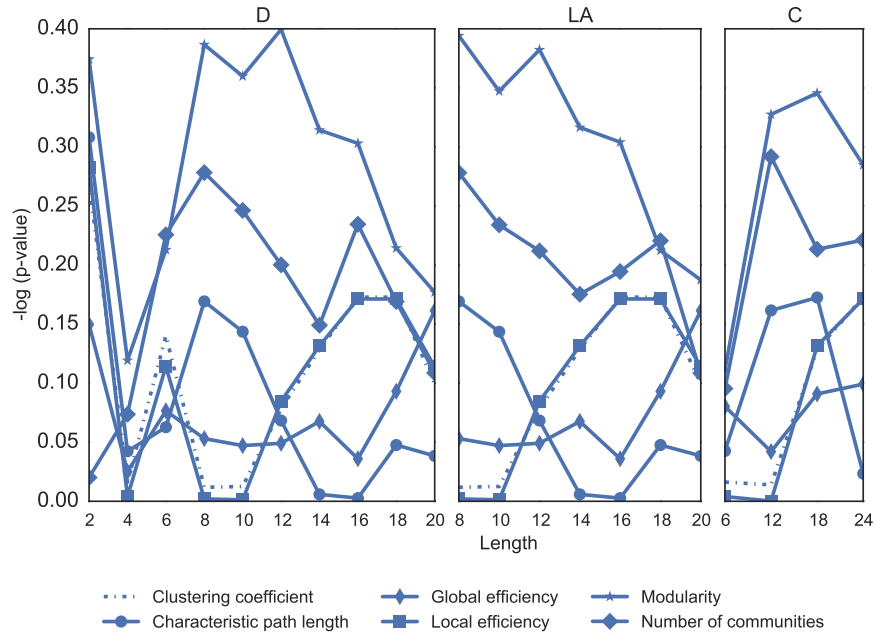


Figure 18: **Effect of Wavelet Filter Type and Length on Statistical Sensitivity in Group Comparisons.** Negative common logarithm of the p -values obtained from two-sample t -tests between diagnostic values extracted from healthy control networks versus those extracted from schizophrenia patient networks. Network diagnostics are calculated for functional brain networks constructed from scale 1 wavelet coefficients. Networks represent the weakest 1% of edges..

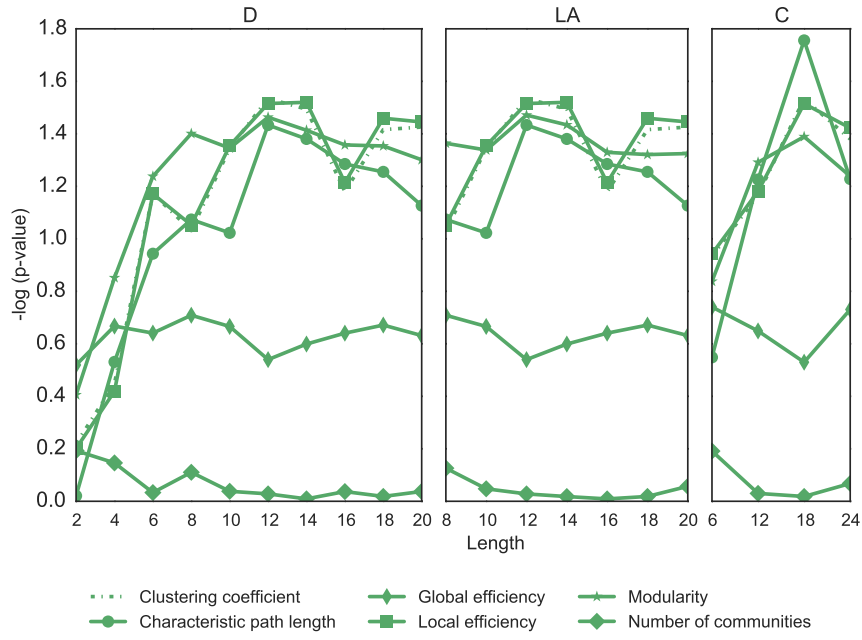


Figure 19: **Effect of Wavelet Filter Type and Length on Statistical Sensitivity in Group Comparisons.** Negative common logarithm of the p -values obtained from two-sample t -tests between diagnostic values extracted from healthy control networks versus those extracted from schizophrenia patient networks. Network diagnostics are calculated for functional brain networks constructed from scale 2 wavelet coefficients. Networks represent the weakest 1% of edges.

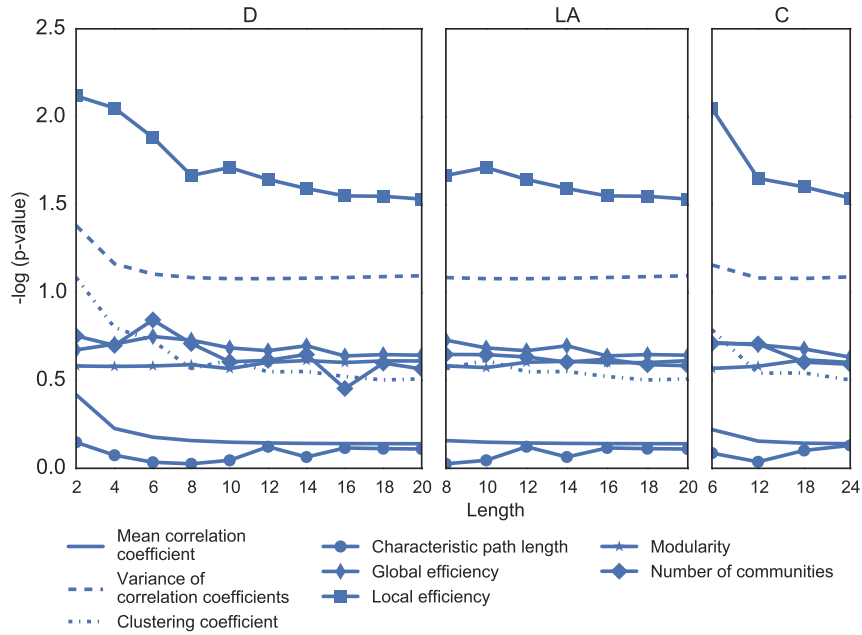


Figure 20: **Effect of Wavelet Filter Type and Length on Statistical Sensitivity in Group Comparisons.** Negative common logarithm of the p -values obtained from two-sample t -tests between diagnostic values extracted from healthy control networks versus those extracted from schizophrenia patient networks. Network diagnostics are calculated for functional brain networks constructed from scale 1 **detail** coefficients. Networks represent the strongest 30% of edges.

References

- Bassett, D. S., Nelson, B. G., Mueller, B. A., Camchong, J., Lim, K. O., 2012. Altered resting state complexity in schizophrenia. *Neuroimage* 59 (3), 2196–2207.
- Grinsted, A., Moore, J. C., Jevrejeva, S., 2004. Application of the cross wavelet transform and wavelet coherence to geophysical time series. *Non-linear processes in geophysics* 11 (5/6), 561–566.
- Schwarz, A. J., McGonigle, J., 2011. Negative edges and soft thresholding in complex network analysis of resting state functional connectivity data. *Neuroimage* 55 (3), 1132–1146.

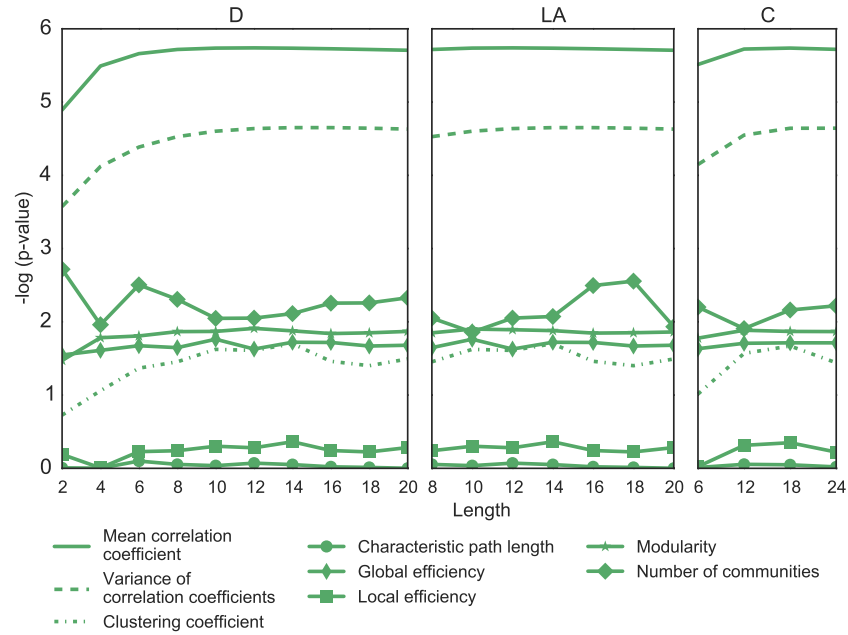


Figure 21: **Effect of Wavelet Filter Type and Length on Statistical Sensitivity in Group Comparisons.** Negative common logarithm of the p -values obtained from two-sample t -tests between diagnostic values extracted from healthy control networks versus those extracted from schizophrenia patient networks. Network diagnostics are calculated for functional brain networks constructed from scale 2 **detail** coefficients. Networks represent the strongest 30% of edges.